

EFFECT OF PEPTIDE HYDROLYSATES FROM RICEBERRY ON REDUCING ENDOPLASMIC
RETICULUM STRESS IN CELLS



A Thesis Submitted in Partial Fulfillment of the Requirements
for the Degree of Master of Science in Green Chemistry and Sustainability

Department of Chemistry

FACULTY OF SCIENCE

Chulalongkorn University

Academic Year 2022

Copyright of Chulalongkorn University

ผลของเพปไทด์ไฮโดรไลเซตจากข้าวไรซ์เบอร์รี่ต่อการลดความเครียดของเอนโดพลาสมิกเรติคูลัมใน
เซลล์



วิทยานิพนธ์นี้เป็นส่วนหนึ่งของการศึกษาตามหลักสูตรปริญญาวิทยาศาสตรมหาบัณฑิต
สาขาวิชาเคมีสีเขียวและความยั่งยืน ภาควิชาเคมี
คณะวิทยาศาสตร์ จุฬาลงกรณ์มหาวิทยาลัย
ปีการศึกษา 2565
ลิขสิทธิ์ของจุฬาลงกรณ์มหาวิทยาลัย

Thesis Title	EFFECT OF PEPTIDE HYDROLYSATES FROM RICEBERRY ON REDUCING ENDOPLASMIC RETICULUM STRESS IN CELLS
By	Miss Theeranuch Jaroenchuensiri
Field of Study	Green Chemistry and Sustainability
Thesis Advisor	CHANAT AONBANGKHEN, Ph.D.

Accepted by the FACULTY OF SCIENCE, Chulalongkorn University in Partial
Fulfillment of the Requirement for the Master of Science

..... Dean of the FACULTY OF SCIENCE
(Professor POLKIT SANGVANICH, Ph.D.)

THESIS COMMITTEE

..... Chairman
(Professor KHANITHA PUDHOM, Ph.D.)

..... Thesis Advisor
(CHANAT AONBANGKHEN, Ph.D.)

..... External Examiner
(Pawin Pongkorpsakol, Ph.D.)

จุฬาลงกรณ์มหาวิทยาลัย
CHULALONGKORN UNIVERSITY

ธีรานุช เจริญชื่นสิริ : ผลของเพปไทด์ไฮโดรไลเซตจากข้าวไรซ์เบอร์รี่ต่อการลดความเครียดของเอนโดพลาสมิกเรติคูลัมในเซลล์. (EFFECT OF PEPTIDE HYDROLYSATES FROM RICEBERRY ON REDUCING ENDOPLASMIC RETICULUM STRESS IN CELLS) อ.ที่ปรึกษาหลัก : ดร.ฉันท อ้นบางเขน

ภาวะเครียดทางออกซิเดชันมีสาเหตุจากการเสียสมดุลระหว่างสารอนุมูลอิสระและสารต้านอนุมูลอิสระซึ่งเป็นปัจจัยในการเกิดโรคต่าง ๆ สารต้านอนุมูลอิสระทางชีวภาพมีความน่าสนใจ ซึ่งอาจมีฤทธิ์ในการยับยั้งการเกิดความเครียดในเอนโดพลาสมิกเรติคูลัม (ER stress) ในงานวิจัยนี้ได้ทำการศึกษาผลของเพปไทด์จากข้าวไรซ์เบอร์รี่ต่อการลด ER stress ภายในเซลล์ เพปไทด์จากข้าวไรซ์เบอร์รี่ทั้ง 10 ชนิดได้รับการทดสอบความเป็นพิษกับเซลล์ L929 และ SH-SY5Y และพบว่าเพปไทด์ทั้งหมดปลอดภัยในการใช้ทดลองกับเซลล์ทั้งสองชนิด อีกทั้งเพปไทด์หมายเลข 3 ถึง 5 และ 10 สามารถปกป้องเซลล์จากภาวะเครียดทางออกซิเดชันที่ถูกกระตุ้นจากกรดไอโอโดอะซิดิก (IAA) และ ไฮโดรเจนเปอร์ออกไซด์ (H_2O_2) นอกจากนี้เพปไทด์ดังกล่าวยังมีคุณสมบัติในการบรรเทาสภาวะ ER stress ในเซลล์ที่ถูกกระตุ้นด้วย tunicamycin (TM) ด้วยการวิเคราะห์ด้วยกล้องจุลทรรศน์ฟลูออเรสเซนซ์โดยใช้ ConA และ Mag-Fluo4 ในการย้อมเซลล์ ผลการทดลองแสดงให้เห็นถึงความเป็นไปได้ของเพปไทด์ของเพปไทด์ในการบรรเทาการเกิด ER stress โดยทำการเปรียบเทียบผลของรูปถ่ายเทียบกับกลุ่มการทดลองของเซลล์ที่ถูกกระตุ้นความเครียดด้วย TM เท่านั้น ผลการทดลองแสดงให้เห็นถึงศักยภาพในการบรรเทาความเครียดใน ER ของเพปไทด์หมายเลข 3 ถึง 5 สามารถลดความเข้มสัญญาณของ ConA และหมายเลข 3 และ 4 มีความเข้มของ Mag-Fluo4 เพิ่มขึ้นเมื่อเทียบกับกลุ่มทดลอง (TM group) แสดงให้เห็นถึงความสามารถของเพปไทด์หมายเลข 3 และ 4 ในการลดการเกิด ER stress การวิเคราะห์สถิติโดยใช้ การวิเคราะห์ความแปรปรวนทางเดียว (One-way ANOVA) ในการยืนยันถึงความแตกต่างที่มีนัยสำคัญ ($p < 0.05$) งานวิจัยนี้ประสบความสำเร็จในการค้นหาเพปไทด์จากข้าวไรซ์เบอร์รี่ที่มีแนวโน้มในการบรรเทาความเครียดใน ER โดยเฉพาะเพปไทด์ 3 และ 4 ที่ควรค่าต่อการศึกษาเพิ่มเติมด้วยวิธีทางอื่นเพื่อยืนยันผลความสามารถดังกล่าว และนำไปประยุกต์ทดลองในสิ่งมีชีวิตเพื่อศึกษากับโรคที่เกี่ยวข้องกับ ER stress

สาขาวิชา เคมีสีเขียวและความยั่งยืน
ปีการศึกษา 2565

ลายมือชื่อนิสิต
ลายมือชื่อ อ.ที่ปรึกษาหลัก

6478033823 : MAJOR GREEN CHEMISTRY AND SUSTAINABILITY

KEYWORD: Peptides, Riceberry rice, Oxidative stress, Endoplasmic reticulum stress,
Antioxidant peptides

Theeranuch Jaroenchuensiri : EFFECT OF PEPTIDE HYDROLYSATES FROM RICEBERRY
ON REDUCING ENDOPLASMIC RETICULUM STRESS IN CELLS . Advisor: CHANAT
AONBANGKHEN, Ph.D.

Oxidative stress, resulting from an imbalance between reactive oxygen species (ROS) and antioxidants, contributes to diseases and induces endoplasmic reticulum (ER) stress. Antioxidants can mitigate ER stress. We investigated synthetic peptides from riceberry rice hydrolysates against ER stress. Ten peptides were evaluated for toxicity and antioxidant activity in SH-SY5Y and L929 cell lines. Peptides ID 3 to ID 5 ,and ID 10 showed significant antioxidant activity protecting cells from oxidative stress induced by IAA and H₂O₂. These peptides alleviated ER stress induced by TM, as observed through fluorescence microscopy analysis using ConA dye. Peptides ID 3 to 5 reduced ConA intensity compared to TM-treated cells, indicating their potential in reducing ER stress. Peptide ID 3 and ID 4 exhibited higher Mag-Fluo4 intensity compared to TM group, signifying its role in controlling calcium ion levels and potentially reducing ER stress. Statistical analysis confirmed significant differences ($p < 0.05$). These findings highlight the antioxidant and ER stress-reducing potential of riceberry peptides, particularly ID 3 and 4. Further investigations are needed to understand their mechanisms and therapeutic applications for managing oxidative- and ER stress-related diseases.

จุฬาลงกรณ์มหาวิทยาลัย
CHULALONGKORN UNIVERSITY

Field of Study: Green Chemistry and
Sustainability

Student's Signature

Academic Year: 2022

Advisor's Signature

ACKNOWLEDGEMENTS

I am deeply grateful to the individuals who have played a significant role in the completion of this project. First and foremost, my heartfelt appreciation goes to my advisor, Dr. Chanat Aonbangkhen, for his invaluable guidance and unwavering support throughout this journey. I extend my sincere thanks to our committee members, Prof. Khanittha Pudhom and Dr. Pawin Pongkorsakon, for their valuable insights and constructive feedback, which greatly enriched this work.

I would like to express my profound gratitude to Dr. Sucheewin Krobthong for generously providing the riceberry-derived peptides and sharing his preliminary results, which were instrumental in the successful execution of our research.

To my dear friends, Kawisara Longsakpreecha, Pichayapa Sukmak, Kriangsak Faikruea, and Kotchakorn Supabowornsathit, your unwavering support and encouragement have been a source of strength and inspiration.

I am grateful to Kriangsak Faikruea, Sutthida Wongsuwan, and my advisor for patiently guiding me in learning the intricacies of cell culture techniques, which proved crucial to the experimental aspects of this study.

To my loving family, I am indebted to your unconditional love, belief in me, and constant encouragement. Your support has been the cornerstone of my journey.

A special thanks goes to Yoshinori from Treasure for his captivating music, which provided solace and motivation during challenging times.

Lastly, I acknowledge and appreciate my own resilience, determination, and unwavering commitment to this endeavor. To all individuals mentioned and those not explicitly named, I am sincerely grateful for your contributions and support throughout this project.

Theeranuch Jaroenchuensiri



จุฬาลงกรณ์มหาวิทยาลัย
CHULALONGKORN UNIVERSITY

TABLE OF CONTENTS

	Page
.....	iii
ABSTRACT (THAI).....	iii
.....	iv
ABSTRACT (ENGLISH).....	iv
ACKNOWLEDGEMENTS.....	v
TABLE OF CONTENTS.....	vii
LIST OF TABLES.....	x
LIST OF FIGURES.....	xi
CHAPTER 1 INTRODUCTION.....	1
CHAPTER 2 LITERATURE REVIEWS.....	6
2.1 Mechanisms of ER Stress and Unfolded Protein Response (UPR).....	7
2.2 Calcium Homeostasis and ER Stress.....	8
2.3 ER-stress inducers used in research.....	9
2.4 The antioxidant peptides from natural sources.....	11
2.5 Exploring the antioxidant potential of riceberry.....	12
2.6 Characterization of antioxidant peptide candidates isolated from riceberry.....	13
2.7 Objective of this research.....	16
CHAPTER 3 EXPERIMENTAL SECTION.....	17
3.1 Materials.....	17
3.1.1 Peptides, Chemicals, and Cell lines.....	17
3.1.2 Water purification.....	18

3.1.3 Analytical Instruments.....	18
3.2 Cell culture	18
3.3 Cell counting.....	19
3.4 MTT assay.....	20
3.5 Chemical preparation for anti-oxidant and anti-ER stress assays	21
3.6 Evaluating toxicity of the synthetic peptides derived from riceberry hydrolysates in cells.....	22
3.7 Measuring the protective effects of peptides on oxidative stress in cells	23
3.8 Fluorescence cell imaging to determine the protective effects on ER-stress by the synthetic peptides from riceberry.....	23
CHAPTER 4 RESULTS AND DISCUSSION.....	26
4.1 The toxicity of the L929 cell line was assessed by testing its response to the standard anticancer drug, Etoposide.	27
4.2 Toxicity of the synthetic peptides derived from riceberry hydrolysates in SH-SY5Y cells	28
4.3 Determining the appropriate concentration of H ₂ O ₂ and IAA to induce oxidative stress in cells (SH-SY5Y cells).....	30
4.4 Assessment of peptide toxicity and evaluation of antioxidant activity in SH-SY5Y cells	33
4.5 Assessment of peptide toxicity and evaluation of antioxidant activity in L929 cells 37	
4.6 Determining the reduction of ER stress in cells via MTT Assay.....	40
4.7 Characterization of ER stress responses in SH-SY5Y and L929 cells using fluorescence imaging	42
4.8 Detecting ER Stress by assessing calcium ion (Ca ²⁺) Levels in the endoplasmic reticulum	63

CHAPTER 5	CONCLUSION.....	74
REFERENCES		76
APPENDIX.....		82
VITA.....		89



LIST OF TABLES

	Page
Table 1 The free radical scavenging activity of all fractions in pH range 3 to 10 obtained from OFFGEL experiment, unpublished data (provided by Dr. Sucheewin Krobthong).....	14
Table 2 Identification of ten candidate peptides from fraction 13 using a de novo algorithm and LC-MS/MS analysis, unpublished data (provided by Dr. Sucheewin Krobthong).....	15
Table 3 Samples ID of the synthetic peptides derived from riceberry hydrolysates... 17	
Table 4 Comparative analysis of peptide effects on ER stress reduction: Descending order of CTCF in L929 and SH-SY5Y cells at different peptide concentrations. (*) denote significant differences compared to TM ($p < 0.05$).	72

LIST OF FIGURES

	Page
Figure 1.1 Signal transduction pathway of ER stress ¹⁸	2
Figure 1.2 Dynamic changes in ER calcium ion levels detected by Mag-Fluo4 during ER stress.	4
Figure 2.1 Comparing the mechanisms of ER Stress and normal cellular conditions....	7
Figure 2.2 The structure of thapsigargin.....	10
Figure 2.3 Mechanism of thapsigargin in inhibiting the SERCA pump.....	10
Figure 3.1 The protocol of cell culture.....	19
Figure 3.2 Example of result by using the automated cell counter.....	20
Figure 3.3 the process of MTT conversion to formazan by NADH-dependent reductases ⁵⁰	20
Figure 3.4 Protocol of MTT assay.....	21
Figure 3.5 The protocol for cell fixation, permeabilization, and staining with ConA and DAPI for fluorescence microscopy.	24
Figure 4.1 Cytotoxicity testing of the standard anticancer drug (Etoposide) in SH-SY5Y and L929 cells. Data are shown as mean \pm SD, n=3.	28
Figure 4.2 Cytotoxicity testing of the A) 25, B) 50, and C) 100 μ g/mL peptide hydrolysates from riceberry rice (SH-SY5Y cells). Data are shown as mean \pm SD, n=329	
Figure 4.3 The conclusion of the results regarding the toxicity of peptides derived from riceberry rice at concentrations of 25, 50, and 100 μ g/mL (SH-SY5Y).....	29
Figure 4.4 Determining the appropriate concentration of A) H ₂ O ₂ and B) IAA to induce oxidative stress in cells (SH-SY5Y cells). Data are shown as mean \pm SD, n=3.....	31
Figure 4.5 Antioxidant activity of riceberry rice peptides at A) 25 B) 50 μ g/mL against IAA 200 μ M C) 25 D) 50 and E) 100 μ g/mL against with IAA 500 μ M (SH-SY5Y).	33

Figure 4.6 Microscopic analysis of SH-SY5Y cellular morphology at 10X magnification A) untreated (healthy cells), B) IAA alone, and C) treated with peptide ID 3 and IAA. 35	
Figure 4.7 Investigating the effectiveness of A) 25 and B) 50 $\mu\text{g}/\text{mL}$ of peptides in mitigating oxidative stress induced by H_2O_2 at a concentration of 500 μM . Data are shown as mean \pm SD, n=3, and (*) denote significant differences compared to H_2O_2 alone (p<0.05). 36	
Figure 4.8 Toxicity of the 50 $\mu\text{g}/\text{mL}$ peptide hydrolysates from riceberry rice (L929 cells). Data are shown as mean \pm SD, n=3. 37	
Figure 4.9 Antioxidant activity of riceberry rice peptides at A) 50 and B) 100 $\mu\text{g}/\text{mL}$ against IAA 500 μM in L929 cells. Data are shown as mean \pm SD, and (*) denote significant differences compared to IAA alone (p<0.05). 38	
Figure 4.10 Investigating the effectiveness of 50 $\mu\text{g}/\text{mL}$ of peptides in mitigating oxidative stress induced by H_2O_2 at a concentration of 500 μM in L929 cells. Data are shown as mean \pm SD, and (*) denote significant differences compared to IAA alone (p<0.05). 39	
Figure 4.11 The protective effects of riceberry rice peptides on ER stress induced by tunicamycin (TM) 20 $\mu\text{g}/\text{mL}$. Data are shown as mean \pm SD, and (*) denote significant differences compared to TM alone (p<0.05). 41	
Figure 4.12 The MTT results obtained using different protocols prior to adding 41	
Figure 4.13 Fluorescence images of (A) L929 cells, and (B) SH-SY5Y cells stained with ConA and DAPI. 42	
Figure 4.14 Fluorescence images of L929 cells were cultured in a cell culture medium without any treatment of peptides or tunicamycin (TM) stained with DAPI (blue) and ConA (green) by DAPI and FITC channel. 43	
Figure 4.15 Fluorescence images of L929 cells treated with TM for 8 h., an inducer of ER stress. 45	
Figure 4.16 Fluorescence images of L929 cells treated with peptides ID 1 to 4 and induced ER stress by TM 10 $\mu\text{g}/\text{mL}$ for 8 h. 46	

Figure 4.17 Fluorescence images of L929 cells treated with peptides ID 5 to 10 at 50 $\mu\text{g}/\text{mL}$ and induced ER stress by TM 10 $\mu\text{g}/\text{mL}$ for 8 h.	47
Figure 4.18 Fluorescence images of L929 cells treated with peptides ID 1 to 6 at 50 $\mu\text{g}/\text{mL}$ and induced ER stress by TM 10 $\mu\text{g}/\text{mL}$ for 16 h.	48
Figure 4.19 Fluorescence images of L929 cells treated with peptides ID 6 to 10 at 50 $\mu\text{g}/\text{mL}$ and induced ER stress by TM 10 $\mu\text{g}/\text{mL}$ for 16 h.	49
Figure 4.20 Morphological analysis of L929 cells treated with peptides exhibiting the worst morphology.	50
Figure 4.21 Morphological analysis and CTCF measurement of L929 cells of peptides ID 3 to 10 at 50 $\mu\text{g}/\text{mL}$ induced by TM 10 $\mu\text{g}/\text{mL}$ for 24 h. A) morphology of L929 cells stained with ConA (FITC channel) and DAPI under fluorescence microscopy (100X magnification).	52
Figure 4.22 Morphological analysis and CTCF measurement of L929 cells treated with peptides ID 3 to 10 at concentrations 50 $\mu\text{g}/\text{mL}$ induced by TM 10 $\mu\text{g}/\text{mL}$ for 24 h. A) morphology of L929 cells stained with ConA (FITC channel) and DAPI under fluorescence microscopy (100X magnification). B) CTCF measurement of ConA intensity in L929 cells ($p < 0.05$).	54
Figure 4.23 Morphological analysis and CTCF measurement of L929 cells treated with peptides ID 3 to 5 at concentrations 100 $\mu\text{g}/\text{mL}$ A) morphology of L929 cells stained with ConA (FITC channel) and DAPI under fluorescence microscopy (100X magnification). B) CTCF measurement of ConA intensity in L929 cells ($p < 0.05$).	56
Figure 4.24 Morphological analysis and CTCF measurement of SH-SY5Y cells treated with peptides ID 3 to 5 at concentrations 50 $\mu\text{g}/\text{mL}$ A) morphology of SH-SY5Y cells stained with ConA (FITC channel) and DAPI under fluorescence microscopy (100X magnification). B) CTCF measurement of ConA intensity in SH-SY5Y cells.	58
Figure 4.25 Morphological analysis and CTCF measurement of SH-SY5Y cells treated with peptides ID 3 to 5 at concentrations 100 $\mu\text{g}/\text{mL}$ A) morphology of SH-SY5Y cells	

stained with ConA (FITC channel) and DAPI under fluorescence microscopy (100X magnification). B) CTCF measurement of ConA intensity in SH-SY5Y cells. 60

Figure 4.26 Quantification of ER stress-induced Ca^{2+} dysregulation using Mag-Fluo4 and CTCF analysis for assessing the protective effects of peptides ID 3 to 5 at 50 $\mu\text{g}/\text{mL}$ of L929 cells induced by TM 10 $\mu\text{g}/\text{mL}$ for 24 h. A) Fluorescence microscopic imaging of ER stress at 100X magnification with FITC and DAPI channels B) CTCF from Mag-Fluo4 intensity ($p < 0.05$). 64

Figure 4.27 Quantification of ER stress-induced Ca^{2+} dysregulation using Mag-Fluo4 and CTCF analysis for assessing the protective effects of peptides ID 3 to 5 at 100 $\mu\text{g}/\text{mL}$ of L929 cells induced by TM 10 $\mu\text{g}/\text{mL}$ for 24 h. A) Fluorescence microscopic imaging of ER stress at 100X magnification with FITC and DAPI channels B) CTCF from Mag-Fluo4 intensity ($p < 0.05$). 66

Figure 4.28 Quantification of ER stress-induced Ca^{2+} dysregulation using Mag-Fluo4 and CTCF analysis for assessing the protective effects of peptides ID 3 to 5 at 50 $\mu\text{g}/\text{mL}$ of SH-SY5Y cells induced by TM 10 $\mu\text{g}/\text{mL}$ for 24 h. A) Fluorescence microscopic imaging of ER stress at 100X magnification with FITC and DAPI channels B) CTCF from Mag-Fluo4 intensity ($p < 0.05$). 69

Figure 4.29 Quantification of ER stress-induced Ca^{2+} dysregulation using Mag-Fluo4 and CTCF analysis for assessing the protective effects of peptides ID 3 to 5 at 100 $\mu\text{g}/\text{mL}$ of SH-SY5Y cells induced by TM 10 $\mu\text{g}/\text{mL}$ for 24 h. A) Fluorescence microscopic imaging of ER stress at 100X magnification with FITC and DAPI channels B) CTCF from Mag-Fluo4 intensity ($p < 0.05$). 71

CHAPTER 1

INTRODUCTION

Riceberry rice has gained recognition as a valuable source of natural antioxidants, offering a safer and edible alternative to synthetic counterparts. Extracted peptides from riceberry rice have demonstrated potent antioxidative activity, effectively reducing cellular oxidative stress¹. Oxidative stress can trigger endoplasmic reticulum (ER) stress, leading to the accumulation of misfolded proteins within the cell². The ER, a vital organelle, governs protein folding, modifications, and the elimination of unfolded proteins during biological processes. It plays a critical role in cellular growth and survival³. ER dysfunction has been implicated in various diseases, including diabetes, neurodegenerative disorders, and inflammation⁴⁻⁷. ER stress has been implicated in the pathogenesis of diabetes, a metabolic disorder affecting millions worldwide. In conditions of chronic nutrient overload and insulin resistance, the ER becomes overwhelmed with misfolded proteins, leading to impaired insulin production and secretion, ultimately contributing to the development of diabetes^{8, 9}. Neurodegenerative disorders, including Alzheimer's disease and Parkinson's disease, also exhibit a strong association with ER stress. Accumulation of abnormal protein aggregates, such as amyloid-beta and alpha-synuclein, within neuronal cells disrupts ER homeostasis, triggering a cascade of events that promote neuronal dysfunction and cell death^{10, 11}.

Furthermore, ER stress has profound effects on cellular growth, survival, and protein folding. Disruptions in ER homeostasis compromise protein folding and quality control processes, leading to the accumulation of misfolded or unfolded proteins. This triggers the unfolded protein response (UPR), a protective cellular response aimed at restoring ER function. However, if the stress is sustained or unresolved, the UPR can induce apoptosis, promoting the elimination of cells that cannot effectively manage ER stress. These cellular responses highlight the intricate relationship between ER stress and cell fate, ultimately influencing tissue homeostasis and disease outcomes^{7, 9, 12, 13}.

The ER, an essential organelle in eukaryotic cells, plays a crucial role in maintaining intracellular homeostasis of calcium levels¹⁴, particularly in protein synthesis and folding. Physiological stressors, such as increased secretory demands or the presence of mutant proteins that cannot fold correctly within the ER, can disrupt the delicate balance between protein folding demands and the ER's folding capacity, leading to ER stress^{4, 15}.

To sense and respond to ER stress, eukaryotic cells have evolved a set of signal transduction pathways known as the unfolded protein response (UPR)¹⁶. Under conditions of ER stress, the UPR is activated to alleviate the burden of unfolded proteins within the ER. This response involves several mechanisms aimed at reducing unfolded protein loading and restoring ER homeostasis. One key mechanism involves signaling to three major UPR branches: IRE1, PERK, and ATF6. Activation of these branches leads to a coordinated response to mitigate ER stress. IRE1 signaling facilitates the expansion of the ER membrane, allowing for increased protein folding capacity and improved protein quality control. PERK activation results in the selective synthesis of key components involved in protein folding, ensuring efficient protein maturation. ATF6 signaling promotes the transcription of genes encoding chaperones and enzymes involved in protein folding and ER-associated degradation (ERAD), further enhancing protein quality control mechanisms (Figure 1.1)^{14, 17, 18}.

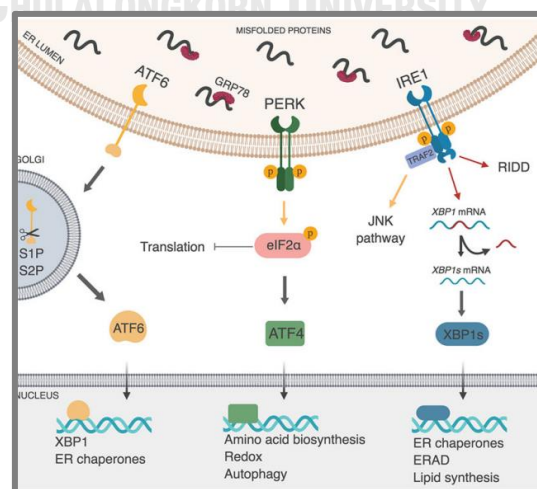


Figure 1.1 Signal transduction pathway of ER stress¹⁸.

Together, these three major branches of the UPR work synergistically to mitigate ER stress and restore protein folding capacity. By expanding the ER, modulating protein synthesis, and enhancing the expression of chaperones and folding enzymes, the UPR aims to alleviate ER stress and promote protein quality control. Understanding the intricate interplay between the UPR branches and their coordinated responses to ER stress is crucial for developing targeted therapeutic interventions aimed at modulating ER homeostasis and ameliorating ER stress-related diseases^{3, 7, 14, 19}.

Calcium homeostasis within the ER is of paramount importance for proper protein folding and chaperone functions. Calcium ions serve as crucial co-factors for various ER-resident chaperones and enzymes involved in protein folding processes. Any disruption in ER calcium levels can lead to the accumulation of misfolded proteins, ultimately triggering ER stress²⁰.

The ER serves as a calcium storage site and is responsible for regulating calcium ion concentrations in the cell, distinct from the calcium levels in the surrounding cytosol. Calcium ions play a vital role in protein folding and chaperone functions within the ER. Disturbances in ER calcium levels can occur due to various factors, including increased secretory demands, the presence of mutant proteins, or altered calcium transport mechanisms. Any decrease in calcium ion levels within the ER can trigger the unfolded protein response (UPR) pathway. This response is mediated by three key transduction proteins, which are involved in signaling and restoring cellular equilibrium^{21, 22}.

To study the impact of calcium levels on ER stress, various techniques and tools have been developed. One such tool is the use of fluorescent calcium indicators, such as Mag-Fluo4. Mag-Fluo4 is a calcium-sensitive dye that can selectively bind to calcium ions especially, in the ER. It enables the measurement of changes in intracellular calcium concentrations, including those within the ER^{21, 23}.

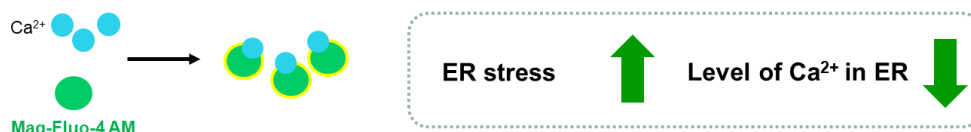


Figure 1.2 Dynamic changes in ER calcium ion levels detected by Mag-Fluo4 during ER stress.

However, if ER stress persists and homeostasis is not restored, the UPR can induce apoptosis, which is a programmed cell death pathway. This serves as a protective mechanism to eliminate cells that cannot effectively manage ER stress. Apoptosis triggered by unresolved ER stress helps maintain cellular integrity and prevents the accumulation of damaged or dysfunctional cells. In addition to detecting changes in calcium ion levels in the ER, cellular morphology and ER morphology can also be used to identify ER stress. When ER stress occurs in cells, it can lead to alterations in cellular shape and structure^{13, 14}. Understanding the role of calcium homeostasis in the ER and its influence on protein folding and the UPR is crucial for comprehending the mechanisms underlying ER stress-related diseases. Further exploration of calcium-sensitive dyes and other tools for monitoring calcium dynamics within the ER will contribute to our understanding of how calcium dysregulation contributes to the development and progression of ER stress-related disorders and may offer potential avenues for therapeutic interventions.

To address the impact of ER stress, this study investigated the protective effects of riceberry rice peptide hydrolysates against ER stress. Ten peptides were evaluated for their toxicity and antioxidant activity using SH-SY5Y and L929 cell lines. The toxicity of the peptides was determined using MTT assays. To assess their antioxidant activity, oxidative stress was induced in the cells using iodoacetic acid (IAA)²⁴ and hydrogen peroxide (H₂O₂)^{25, 26}.

By subjecting the cells to oxidative stress, the study aimed to measure the ability of the peptides to protect the damaging effects of reactive oxygen species (ROS) and reduce oxidative stress. Antioxidants play a crucial role in neutralizing ROS and protecting cells from oxidative damage²⁷. Therefore, the evaluation of

antioxidant activity in the presence of oxidative stress provides valuable insights into the potential of the riceberry rice peptides to mitigate ER stress.

By examining the toxicity and antioxidant activity of the ten peptides, this study aims to identify peptides that exhibit significant antioxidant properties, effectively protecting cells from oxidative stress induced by IAA and H₂O₂. Peptides ID 3, 4, 5 and 10 demonstrated significant antioxidant activity. Subsequently, the potential of these peptides to alleviate ER stress induced by tunicamycin (TM) was assessed.

Fluorescence microscopy analysis revealed changes in the cell morphology and the intensity of ER-localized dye, concanavalin A (ConA), suggesting a potential reduction in ER stress. Peptides ID 3, 4, and 5 exhibited a significant decrease in ConA intensity compared to the TM-treated group, indicating their potential in reducing ER stress. Particularly, peptide ID 3 displayed the highest intensity of Mag-Fluo4, a calcium-sensitive dye used to detect calcium ion levels in the ER. This suggests its role in controlling calcium ion levels and potentially reducing ER stress. These findings emphasize the antioxidant and ER stress-reducing potential of riceberry rice peptides, with peptide ID 3 showing promising results. Further investigations are warranted to clarify the mechanisms underlying these effects and explore their therapeutic applications in managing oxidative and ER stress-related disease.

CHAPTER 2

LITERATURE REVIEWS

The L929 cell line has been widely used to study cell viability and cytotoxicity in response to various agents. On the other hand, the SH-SY5Y cell line, derived from a neuroblastoma patient, exhibits neuronal-like characteristics and has been extensively utilized in neurobiological and neuropharmacological research, particularly for studying neurodegenerative disorders such as Parkinson's and Alzheimer's diseases^{28, 29}. These cell lines provide valuable models for investigating cellular processes, disease mechanisms, and potential therapeutic interventions. The L929 cells are useful for assessing general cell viability and cytotoxicity, while the SH-SY5Y cells allow researchers to study neuronal development, function, and disease-related processes.

Over the past few years, there has been a growing interest in exploring the potential of plant metabolites as therapeutic agents for modulating ER stress and exhibiting antioxidant activity. Elevated levels of reactive oxygen species (ROS) disrupt the balance between oxidants and antioxidants in cells, resulting in oxidative stress^{27, 30, 31}. This oxidative stress can subsequently trigger ER stress, which is characterized by the accumulation of misfolded proteins within the endoplasmic reticulum (ER)^{2, 17}. The ER is a vital organelle responsible for protein folding, modification, and quality control processes, crucial for cellular homeostasis, growth, and survival^{3, 32}. Perturbations in ER function are implicated in several diseases, including diabetes, neurodegenerative disorders, inflammation, and cardiovascular conditions³⁻⁵. In recent years, numerous plant-derived metabolites have been identified as potent antioxidants, offering promising therapeutic potential. These metabolites, present in various plant sources such as tomatoes³³, cinnamon³⁴, and lingzhi mushrooms³⁵, have demonstrated antioxidant properties and are utilized in modern medicine.

Moreover, the research has demonstrated the effects of bioactive compounds found in mushrooms, including *Pleurotus ostreatus*, *Ganoderma lucidum*, and *Ustilago maydis*, in reducing ER stress in cells. These mushrooms have been found to contain a variety of bioactive components, such as polysaccharides, phenolic compounds, and other phytochemicals, which contribute to their therapeutic properties³⁶.

However, the investigation of bioactive peptides derived from riceberry rice, an important crop in Thailand, remains relatively unexplored. Riceberry rice is known to contain a plethora of natural antioxidants¹, and previous studies have indicated the presence of bioactive peptides with antioxidant activity. This raises the hypothesis that these peptides may possess the ability to mitigate ER stress in cells, in addition to their antioxidant properties. Before commencing the experimental investigation, it is essential to establish a comprehensive understanding of the underlying processes and implications associated with ER stress.

2.1 Mechanisms of ER Stress and Unfolded Protein Response (UPR)

Under normal conditions, the three transducers on the ER, including IRE1, PERK, and ATF6, exist in an inactive form as they are bound to GRP78.

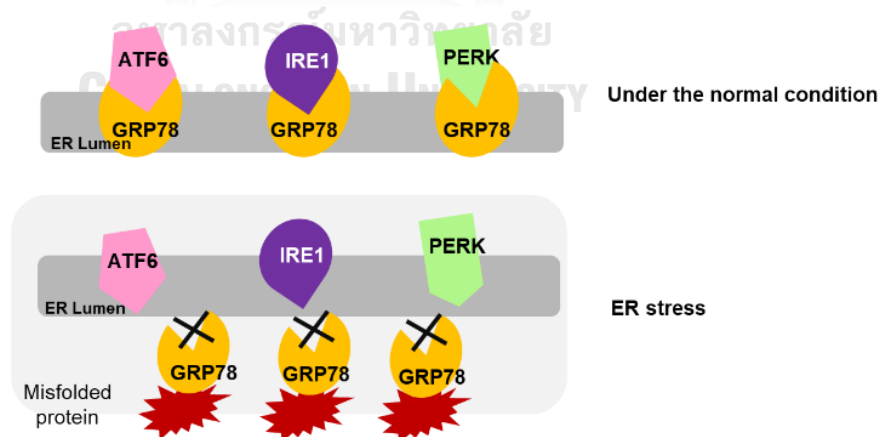


Figure 2.1 Comparing the mechanisms of ER Stress and normal cellular conditions.

During ER stress, these transducers are activated as GRP78 is disrupted by misfolded proteins, preventing their binding to the transducers (Figure 2.1). This association ensures the maintenance of ER homeostasis and prevents the activation of the UPR. However, during ER stress, an accumulation of misfolded proteins occurs within the ER lumen, leading to the disruption of GRP78 binding to the transducers. This release of GRP78 allows for the activation of the UPR signaling pathways mediated by IRE1, PERK, and ATF6³⁷.

- **ATF6** was activated by ER stress, causing its translocation to the Golgi apparatus where it is proteolytically cleaved. The cleaved ATF6 fragment enters the nucleus and acts as a transcription factor, promoting the expression of genes involved in ER protein folding, ERAD, and lipid metabolism³⁸.
- **IRE1** is activated and acts as both a sensor and an effector of the UPR. It undergoes autophosphorylation and splices the X-box binding protein 1 (XBP1) mRNA, leading to the production of spliced XBP1 (XBP1s). XBP1s is a transcription factor that upregulates genes involved in protein folding, ER-associated degradation (ERAD), and ER expansion^{17, 39}.
- **PERK** activated PERK phosphorylates eukaryotic translation initiation factor 2 alpha (eIF2 α), leading to global translational attenuation. This reduces the protein load entering the ER, allowing the cell to cope with ER stress⁴⁰.

2.2 Calcium Homeostasis and ER Stress

High concentration of calcium ion in ER is play an important role in protein folding and quality control. Calcium ions act as cofactors for numerous ER-resident chaperones and enzymes involved in protein maturation and folding processes. These include protein disulfide isomerases (PDIs)⁴¹, calreticulin, and calnexin, which facilitate the formation of correct disulfide bonds and promote proper protein

folding⁴². Indeed, the use of Mag-Fluo4 to detect alterations in calcium ion levels in the endoplasmic reticulum (ER) is a well-established technique. In situations where ER stress is induced, such as through the accumulation of misfolded proteins or disruption of protein folding processes, it can lead to perturbations in calcium homeostasis within the ER. Under normal conditions, the ER maintains a low concentration of free calcium ions. However, during ER stress, calcium is released from the ER stores, leading to an increase in cytosolic calcium levels and a decrease in calcium levels within the ER lumen. This alteration in calcium ion levels can be visualized and quantified using calcium-sensitive dyes like Mag-Fluo4^{21, 23}.

Mag-Fluo4 is a fluorescent calcium indicator that exhibits increased fluorescence intensity upon binding to calcium ions. Therefore, a decrease in the intensity of Mag-Fluo4 fluorescence indicates a reduction in ER calcium levels, which is commonly observed during ER stress. By monitoring the changes in Mag-Fluo4 fluorescence, researchers can assess the impact of various factors, such as peptide treatments or cellular stressors, on ER calcium homeostasis. This allows for the investigation of potential protective effects or interventions aimed at restoring normal calcium levels and mitigating ER stress-induced cellular dysfunction.

2.3 ER-stress inducers used in research

The two main ER stressors that are commonly used to activate the Unfolded Protein Response (UPR) pathway. These stressors play a crucial role in inducing ER stress and triggering the cellular response to unfolded or misfolded proteins.

- **Thapsigargin** is a potent and selective inhibitor of the sarco/endoplasmic reticulum Ca^{2+} -ATPase (SERCA) pump. It effectively depletes intracellular calcium stores by blocking the reuptake of calcium into the endoplasmic reticulum (ER). The reduction in calcium levels triggers the unfolded protein response (UPR) and ER stress (Figure 2.3)⁴³. Thapsigargin has been widely

used as a pharmacological tool to induce ER stress and investigate its effects on cellular processes.

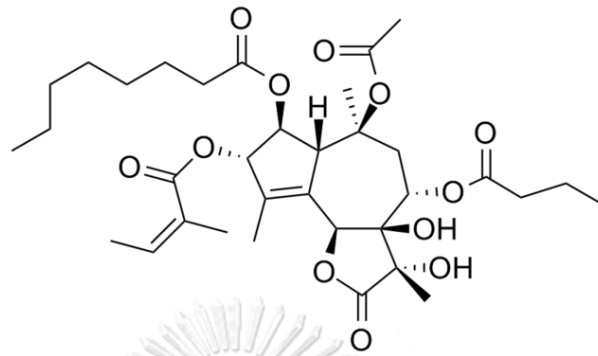


Figure 2.2 The structure of thapsigargin.

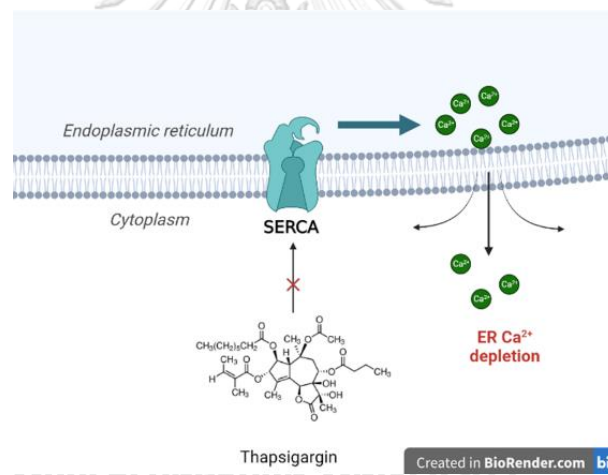


Figure 2.3 Mechanism of thapsigargin in inhibiting the SERCA pump.

- **Tunicamycin (TM)** is a commonly used ER stress inducer that specifically inhibits N-linked glycosylation, an essential process for protein folding and quality control in the ER. By blocking N-linked glycosylation, tunicamycin disrupts proper protein folding, leading to the accumulation of misfolded proteins and triggering the unfolded protein response (UPR)^{44, 45}.

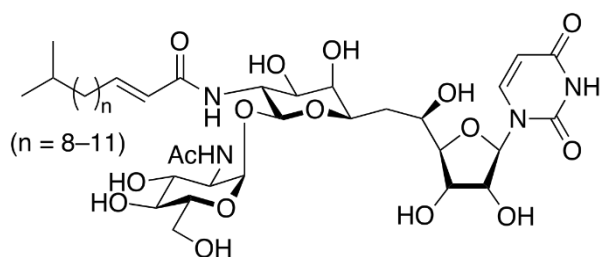


Figure 2.1. The structure of tunicamycin (TM).

Both Tunicamycin and Thapsigargin disrupt calcium ion levels in the ER, ultimately inducing ER stress and triggering downstream cellular responses. The specific mechanisms by which these compounds impact calcium homeostasis and induce ER stress may vary, but their overall effect on calcium ion levels is similar²¹.

2.4 The antioxidant peptides from natural sources

Several studies have investigated the antioxidant activity of peptides derived from various sources. For instance,

1. Peptides derived from *Ganoderma lucidum* and found that three out of seven synthetic peptides exhibited *in vitro* antioxidant activity. These peptides effectively suppressed intracellular reactive oxygen species (ROS) levels. The peptides sequence, VDLPTC³⁵ and NH₂-PVRSSNCA-CO₂H (octapeptide)⁴⁶ demonstrated the highest antioxidant capacity and significant suppression of intracellular ROS levels.
2. The peptides derived from *Tecoma stans* (L.), a well-known medicinal plant found in tropical regions, has the antioxidant properties⁴⁷.
3. Legumes such as soybean, chickpea, lentil, cowpea, and mung bean have also been investigated for their potential antioxidative activities. Protein hydrolysates derived from these legumes have shown promising antioxidant activities⁴⁸.

These studies collectively demonstrate the potential of various peptides, derived from different sources, to exhibit antioxidant properties. The identification and characterization of antioxidant peptides from natural sources contribute to the understanding of their health-promoting effects and may have implications in the development of functional food products with enhanced antioxidant capabilities. Indeed, while there have been studies examining the antioxidant activity of peptides derived from various sources, there is only little research focusing on the effects of antioxidant peptides in reducing endoplasmic reticulum (ER) stress. Therefore, our study aims to fill this research gap by investigating the potential of peptides derived from riceberry to not only exhibit antioxidant properties but also mitigate ER stress in cells.

2.5 Exploring the antioxidant potential of riceberry

The antioxidant properties of riceberry rice have been extensively investigated in recent studies. Settapramote et al. (2021) conducted a study specifically focusing on the antioxidant potential of anthocyanins, which are abundant in riceberry rice. Their research involved extracting these antioxidant compounds and evaluating their effectiveness against oxidative stress. The findings strongly support the notion that anthocyanins contribute significantly to the antioxidant activity of riceberry rice, highlighting its potential health benefits.

Prangthip et al. (2013) studied the effects of dark purple riceberry, known for its higher dietary fiber and antioxidant content. The researchers utilized riceberry supplement (RB) to assess its impact on various parameters related to oxidative stress, inflammation, and metabolic disorders in diabetic rats. The results revealed significant improvements in blood glucose levels, insulin sensitivity, oxidative stress markers, antioxidant enzyme activity, and inflammatory cytokines. Moreover, histological improvements in the pancreas and spleen further supported the potential of RB in alleviating hyperglycemia, hyperlipidemia, and oxidative stress while reducing inflammation.

Including these studies provides valuable insights into the antioxidant properties of riceberry rice and its potential therapeutic effects. These findings underscore the importance of incorporating riceberry rice into the diet to harness the antioxidant benefits and mitigate various health conditions associated with oxidative stress.

2.6 Characterization of antioxidant peptide candidates isolated from riceberry

Based on the previous unpublished work by Dr. Sucheewin Krobthong, he extracted peptide hydrolysates and identify peptide sequences that showed the antioxidant activity via DPPH and ABTS assay. After discovering ten peptides with antioxidant properties, we purchased these peptides from GenScript Biotech Corporation.

To identify and isolate peptides with antioxidant activity from riceberry, Dr. Sucheewin used a chromatographic technique called OFFGEL. This method separated the peptides from riceberry into 18 distinct fractions (Table 1). Among these fractions, fraction 13 exhibited the highest antioxidant activity as determined by the DPPH and ABTS assays. To determine the sequence of peptides in this fraction, Dr. Sucheewin employed a de novo algorithm in conjunction with LC-MS/MS analysis. Through these techniques, he successfully identified and characterized 10 peptides from riceberry that possess confirmed antioxidant properties (Table 2).

Table 1 The free radical scavenging activity of all fractions in pH range 3 to 10 obtained from OFFGEL experiment, unpublished data (provided by Dr. Sucheewin Krobthong).

Fraction	pH range	Antioxidant capacity	
		DPPH (IC ₅₀) ($\mu\text{g/mL}$)	ABTS (IC ₅₀) ($\mu\text{g/mL}$)
Fraction 1	3.000–3.389	90.21 ^p ±0.13	66.37 ^p ±0.15
Fraction 2	3.389–3.778	98.42 ^o ±0.22	60.23 ^o ±0.07
Fraction 3	3.778–4.167	89.13 ⁿ ±0.17	63.21 ⁿ ±0.19
Fraction 4	4.167–4.556	66.22 ^m ±0.07	54.38 ^m ±0.25
Fraction 5	4.556–4.944	72.52 ^l ±0.16	59.32 ^l ±0.13
Fraction 6	4.944–5.333	80.07 ^k ±0.11	61.81 ^k ±0.12
Fraction 7	5.333–5.722	61.90 ^j ±0.07	43.12 ^j ±0.05
Fraction 8	5.722–6.111	63.81 ⁱ ±0.19	45.30 ⁱ ±0.09
Fraction 9	6.111–6.500	55.69 ^h ±0.08	54.73 ^h ±0.17
Fraction 10	6.500–6.889	22.44 ^g ±0.01	29.92 ^g ±0.12
Fraction 11	6.889–7.278	18.83 ^f ±0.07	25.34 ^f ±0.09
Fraction 12	7.278–7.667	45.42 ^e ±0.06	32.15 ^e ±0.16
Fraction 13	7.667–8.056	12.31 ^d ±0.08	21.69 ^d ±0.13
Fraction 14	8.056–8.444	57.33 ^c ±0.21	40.23 ^c ±0.19
Fraction 15	8.444–8.833	43.21 ^b ±0.11	32.73 ^b ±0.10
Fraction 16	8.833–9.222	49.80 ^a ±0.17	34.89 ^a ±0.08
Fraction 17	9.222–9.611	NA	NA
Fraction 18	9.611–10.000	NA	NA

Table 2 Identification of ten candidate peptides from fraction 13 using a de novo algorithm and LC-MS/MS analysis, unpublished data (provided by Dr. Sucheewin Krobthong).

Peptide ID	Peptide sequence	Molecular weight (Da)
ID 1	PEHYLDHFKL	1297.65
ID 2	FYDPKTPFF	1160.55
ID 3	VPAGVAHW	835.43
ID 4	LKELGDKVPAPVKE	1521.88
ID 5	LDDPAKKLVFEGGSA	1416.76
ID 6	PASVAHW	766.38
ID 7	LDDPAKKLVF	1144.65
ID 8	AKLPPGSD	783.41
ID 9	TLKYPLE	862.48
ID 10	DVHSHASN	964.44

In our study, we are curious to know if these peptides also have the ability to act as antioxidants and reduce ER stress in cells.

2.7 Objective of this research

1. To evaluate the possible protective effects of peptide hydrolysates from riceberry (*Oryza sativa*) on endoplasmic reticulum (ER) stress in cells
2. To obtain peptide hydrolysates from riceberry (*Oryza sativa*) for good health and well-being



CHAPTER 3

EXPERIMENTAL SECTION

3.1 Materials

3.1.1 Peptides, Chemicals, and Cell lines

- Ten synthetic peptides derived from riceberry hydrolysates were ordered from GenScript Biotech Corporation.

Table 3 Samples ID of the synthetic peptides derived from riceberry hydrolysates.

Peptide ID	Sequences
ID 1	PEHYLDHFKL
ID 2	FYDPKTPFF
ID 3	VPAGVAHW
ID 4	LKELGDKVPAPVKE
ID 5	LDDPAKKLVEGGSA
ID 6	PASVAHW
ID 7	LDDPAKKLVF
ID 8	AKLPPGSD
ID 9	TLKYPLE
ID 10	DVVHSHASN

- L929 cell line, a normal cell line, was obtained from professor Tanapat Palaga (TP) lab at Chulalongkorn University.
- SH-SY5Y cell line, a neuroblastoma cell line, was obtained from James Walker lab at Harvard University.
- Dulbecco's modified Eagle's medium (Cat.no. :1TFS-1CC-12800082, fetal bovine serum (FBS) (Cat.no. :1TFS-1RS-A5256701), 0.05% trypsin-EDTA

(Cat.no. :1TFS-1CC-25300062), and penicillin streptomycin (Cat.no. :1TFS-1CC-15140122) were purchased from Gibco (Grand Island, NY, USA).

- MTT (3-(4,5- Dimethyl-2-thiazolyl)-2,5-diphenyl) (Cat.no. :M6494), dimethyl sulfoxide (DMSO) (Cat.no. :D139-1), concanavalin A (ConA) (Cat.no. :C860), DAPI (Cat.no. :D21490), and Mag-Fluo4AM (Cat.no. :M14206) were purchased from Fisher Scientific (Loughborough, UK).
- Tunicamycin (TM) (Cat.no. :T7765-5MG) was purchased from Merck (Darmstadt, Germany).

3.1.2 Water purification

- Ultrapure water was obtained using a Mili-Q water purification system from Merck (Darmstadt, Germany).

3.1.3 Analytical Instruments

- Automated cell counter (Invitrogen the Countess 3 model), was obtained from Thermo Fisher Scientific (Loughborough, UK).
- The microplate reader (Perkin Elmer Ensign) was used for the MTT assay was purchased from Perkin Elmer (Waltham, MA, USA).
- Fluorescence images were captured using a fluorescence microscope from ZEISS (Oberkochen, Germany).

3.2 Cell culture

SH-SY5Y and L929 cells were cultured in a sterile environment using specific growth media. SH-SY5Y cells were cultured in DMEM/F-12 (Dulbecco's Modified Eagle Medium/Nutrient Mixture F-12), while L929 cells were cultured in Dulbecco's Modified Eagle's Medium (DMEM). Both media were supplemented with 10% fetal bovine serum (FBS) and 1% penicillin/streptomycin. The cells were maintained at a temperature of 37°C in a humidified atmosphere containing 5% CO₂ to provide optimal conditions for their growth and viability.

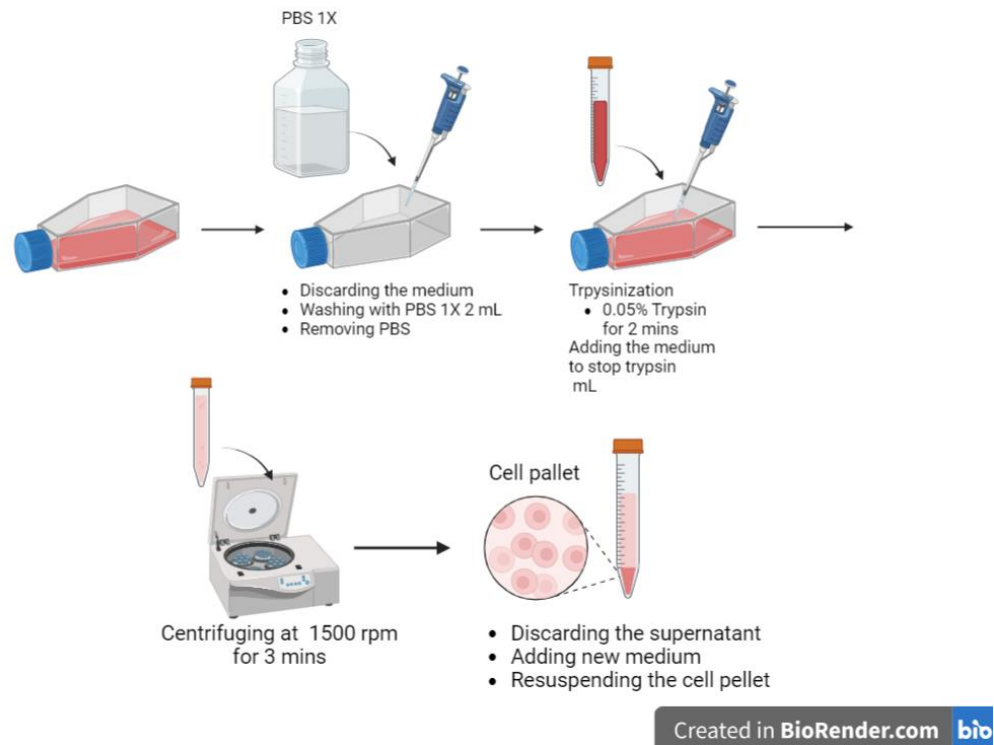


Figure 3.1 The protocol of cell culture.

3.3 Cell counting

For cell counting, first, transfer 10 μL of the cells into a microcentrifuge tube. Mix the cells with 10 μL of trypan blue solution, ensuring thorough mixing to facilitate cell staining. Next, take 10 μL of the mixed cell and trypan blue solution and place it on a counting slide. Carefully cover the slide with a cover glass to create a suitable environment for cell visualization. Once the slide is prepared, perform the cell counting using an automated cell counter. Follow the instructions provided by the instrument for loading the slide and initiating the counting process. The automated cell counter will analyze the cells and provide results such as cell concentration and viability (live cells). Cells with a viability of above 90% are considered suitable for further experimentation.



Figure 3.2 Example of result by using the automated cell counter.

3.4 MTT assay

The MTT assay is a widely used colorimetric method for assessing cytotoxicity and cell viability. In this assay, the yellow tetrazolium salt called MTT (3-(4,5-dimethylthiazol-2-yl)-2,5-diphenyltetrazolium bromide) is reduced by the metabolic activity of viable cells, resulting in the formation of purple formazan crystals (Error! Reference source not found.)^{49, 50}.

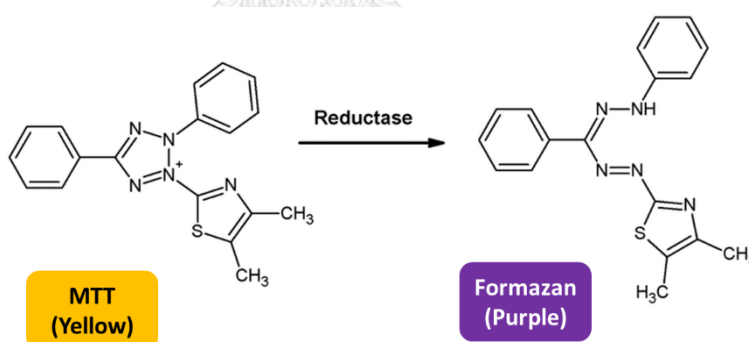


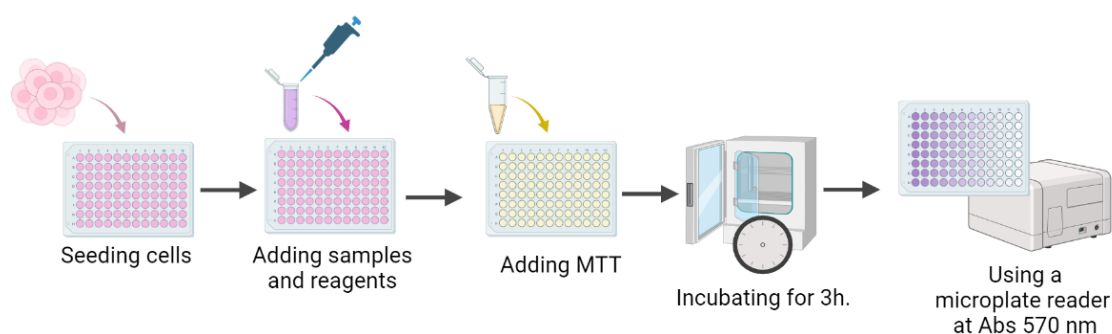
Figure 3.3 the process of MTT conversion to formazan by NADH-dependent reductases⁵⁰.

To prepare the MTT solution, first, weigh approximately 0.100 g of MTT powder. Dissolve the weighed MTT powder in 20.0 mL of distilled water (H₂O) into a concentration at 0.500 mg/mL and transfer it to a suitable container. Use a sonicator to sonicate the MTT solution until it becomes a homogeneous solution, ensuring that

all the MTT powder is fully dissolved. To dilute, the MTT solution will result in a final concentration of 5.00 µg/mL for the MTT solution in the culture medium.

The cells were seeded onto a 96-well plate at a density of 10,000 cells per well and incubated at 37°C in a 5% CO₂ atmosphere for one day. After incubation, the cells were treated with peptides at selecting concentrations for 1 day, as well as with reagents such as 200 and 500 µM IAA, 500 µM H₂O₂, and 20 µg/mL of TM, which were pre-equilibrated for a suitable time incubation. In the following step, the MTT solution was added in the plates 10 µL/well incubated for 3 h. The plates were discarded the medium and MTT, and the formazan was dissolved by DMSO 100 µL/well. The plate was measured the absorbance (Abs) at 570 nm by a microplate reader. The percentage of viability was carried out with equation (1).

$$\%Viability = \frac{\text{Abs of sample}}{\text{Abs of negative control}} \times 100\% \quad \text{--- (1)}$$



Created in [BioRender.com](https://www.biorender.com)

Figure 3.4 Protocol of MTT assay.

3.5 Chemical preparation for anti-oxidant and anti-ER stress assays

For the preparation of a stock solution, 1 mg of the peptide was dissolved in 1 mL of sterilized Mili-Q water, which is type 1 water. The stock solution was then

stored at -20°C for future use. For routine experiments, the stock solution was further diluted in a culture medium to obtain final concentrations of 25, 50, and 100 $\mu\text{g}/\text{mL}$.

To prepare the solution for the culture medium, the stock of 6% hydrogen peroxide (H_2O_2) and iodoacetic acid (IAA) was first dissolved in sterilized water. The resulting solution was then further diluted in the culture medium to the desired concentration. Similarly, the stock solution of tunicamycin (TM) with a concentration of 5 mg/mL and Etoposide were dissolved in filtered dimethyl sulfoxide (DMSO). The DMSO stock solution was then diluted in the culture medium to achieve the desired concentration for the experiments.

3.6 Evaluating toxicity of the synthetic peptides derived from riceberry hydrolysates in cells

L929 or SH-SY5Y cells were seeded in a 96-well plate at a density of approximately 10,000 cells per well. The cells were then treated with different concentrations (25, 50, or 100 $\mu\text{g}/\text{mL}$) of peptides, which were diluted in a culture medium, for a duration of 24 h. After the incubation period, the peptides were removed from the wells. To evaluate the cytotoxicity of the peptides, an MTT assay was performed. The negative control consisted of wells containing only cells in a culture medium, without any peptide treatment. The absorbance of the formazan product, proportional to the number of viable cells, was measured at a wavelength of 570 nm using a microplate reader. This allowed for the determination of the cytotoxic effects of the peptides on the L929 or SH-SY5Y cells.

By comparing the absorbance values of the treated cells with those of the negative control, the relative cell viability and potential cytotoxicity of the peptides at different concentrations could be assessed.

3.7 Measuring the protective effects of peptides on oxidative stress in cells

In the evaluation of the toxicity and protective effects of peptide hydrolysates from riceberry rice, the peptides were diluted in a culture medium to achieve a final concentration of 25, 50, or 100 $\mu\text{g/mL}$, following the methodology outlined in the previous study. The cells, either L929 or SH-SY5Y, were seeded in a 96-well plate, allowing them to attach and grow for 24 h. Subsequently, the diluted peptide hydrolysates were added to the cells and incubated for 24 h. Following the incubation, the peptide hydrolysates were removed, and the cells were subjected to oxidative stress induction using IAA and H_2O_2 at a selecting concentration for a specified duration, such as 3 h. for IAA and 24 h. for IAA. To assess the viability of the cells with the MTT assay as described in the previous study. The controls are untreated with oxidative stressor (cells with only a cell culture medium) and treated with oxidative stressors. The percentage of viability was carried out with the formula as shown in part of MTT assay, equation (1).

3.8 Fluorescence cell imaging to determine the protective effects on ER-stress by the synthetic peptides from riceberry

L929 or SH-SY5Y cells were seeded in 8-well chamber slides at a density of approximately 50,000 cells per well. The peptides, at various concentrations, were pre-treated and added to the cells along with tunicamycin (TM) at a concentration of 10 $\mu\text{g/mL}$ for 24 h.

To prepare the cells for imaging, the cells were fixed and permeabilized using a solution of 4% paraformaldehyde for 15 mins, followed by treatment with Triton X-100 for 2 mins to ensure proper cell permeabilization. Subsequently, the cells were stained with concanavalin A (ConA) and DAPI (at a concentration of 1 $\mu\text{g/mL}$) to visualize specific cellular structures.

The cellular morphology and staining patterns were observed using a fluorescence microscope. The negative control consisted of cells treated with a 1% DMSO solution in the culture medium (as TM was dissolved in DMSO). The positive control of TM alone involved cells treated with 10 $\mu\text{g}/\text{mL}$ of TM, which was diluted in the culture medium.

For live cell staining with Mag-Fluo4 AM, a different protocol was followed compared to the staining with ConA and DAPI. After treating the cells with tunicamycin (TM), the Mag-Fluo4 AM dye was diluted in a culture medium to achieve a final concentration of 6 μM . The dye solution was added to the cells and incubated for 30 mins. Following incubation, the cells underwent the same procedures of cell fixation and permeabilization as described in the preparation of cells for imaging, which involved treating the cells with fixation, such as paraformaldehyde for 15 mins, and permeabilizing them with Triton X-100 for 2 mins.

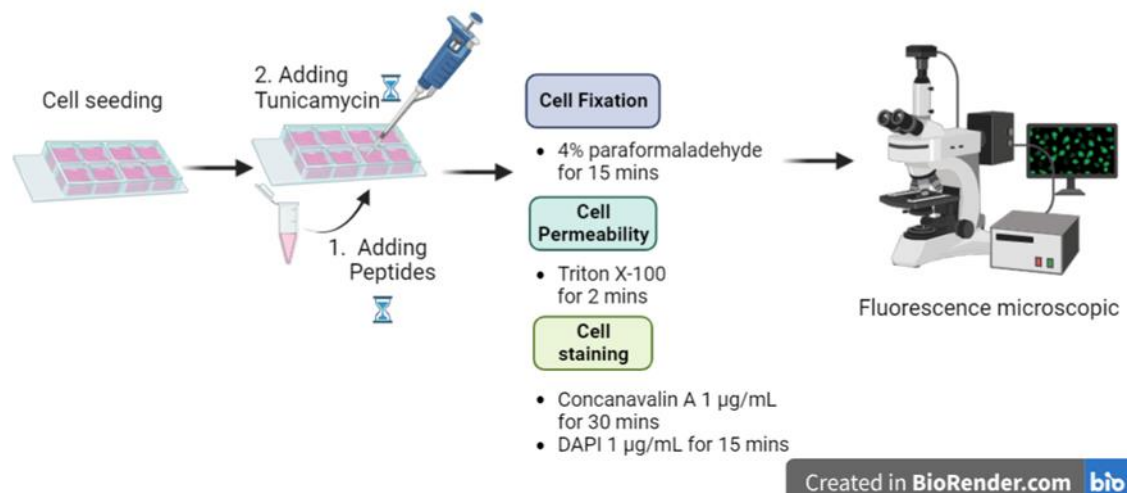


Figure 3.5 The protocol for cell fixation, permeabilization, and staining with ConA and DAPI for fluorescence microscopy.

In our experimental study, we employed the corrected total cell fluorescence (CTCF) method to calculate the fluorescence intensity⁵¹ associated with two different fluorescent probes: ConA (Concanavalin A) and Mag-Fluo4.

CTCF= Integrated Density – (Area of selected cell x Mean fluorescence of background readings) (2)



CHAPTER 4

RESULTS AND DISCUSSION

Endoplasmic reticulum (ER) plays important role in protein folding in cells or protein homeostasis. Accumulation of unfolded proteins in cell organisms can instigate ER stress that is involved in many diseases such as metabolic, cardiovascular, and neurodegenerative diseases like Alzheimer's and Parkinson's⁴⁻⁶. Consequently, reducing ER stress is crucial and important. Strikingly, antioxidant treatments are very effective in the treatment of diseases associated with oxidative stress in reducing reactive oxygen species (ROS)²⁷. ER stress and oxidative stress are related process that play critical roles in cellular homeostasis and function. The accumulation of misfolded proteins in ER stimulates oxidative stress in cells². The ER, a vital organelle, governs protein folding, modifications, and the elimination of unfolded proteins during biological processes. It plays a critical role in cellular growth and survival³.

Riceberry rice, a popular variety of rice derived from the crossbreeding of Thai jasmine rice (Khao Dawk Mali 105) and Thai purple rice (Hom Nil), has gained considerable attention due to its potential health benefits. It is known for its rich antioxidant content, which is attributed to the presence of bioactive compounds such as phenolic compounds, flavonoids, and anthocyanins. These compounds have been associated with various health-promoting effects, including their ability to combat oxidative stress¹. Assuming that the peptides have a protective effect on reducing ER stress, the peptides could be used as supplements in food for good health and well-being in the future.

In our experimental study, we aimed to assess the potential of synthetic peptides derived from riceberry rice in reducing ER stress. To achieve this, we employed several techniques and assays to evaluate different aspects of peptide

activity. Firstly, we conducted toxicity tests using the synthetic peptides to determine their safety profile. This step was crucial to ensure that the peptides did not exert harmful effects on the cells. Next, we performed an antioxidant activity assessment through the MTT assay. This assay allowed us to evaluate the ability of the peptides to counteract oxidative stress, a common trigger for ER stress. To further investigate the impact of the peptides on ER stress, we utilized fluorescence microscopy to observe the morphology of the ER in cells. Changes in ER morphology, such as alterations in shape, intensity, and distribution, can indicate the presence of ER stress. By examining the cells under fluorescence microscopy, we aimed to determine whether the synthetic peptides derived from riceberry could influence the ER morphology and potentially alleviate ER stress. Additionally, we employed the Mag-Fluo4, Ca^{2+} indicator to measure intracellular Ca^{2+} levels in ER. Ca^{2+} depletion is a significant consequence of ER stress. By quantifying Ca^{2+} levels in the presence of the synthetic peptides, we aimed to validate their ability to alleviate ER stress by preventing Ca^{2+} imbalance.

4.1 The toxicity of the L929 cell line was assessed by testing its response to the standard anticancer drug, Etoposide.

MTT assay was employed to assess cell viability. Before testing the samples, a validation step was conducted using the standard drug etoposide. This pre-testing with etoposide served to establish a baseline response and ensure the accuracy and reliability of the assay by confirming its sensitivity and ability to detect changes in cell viability.

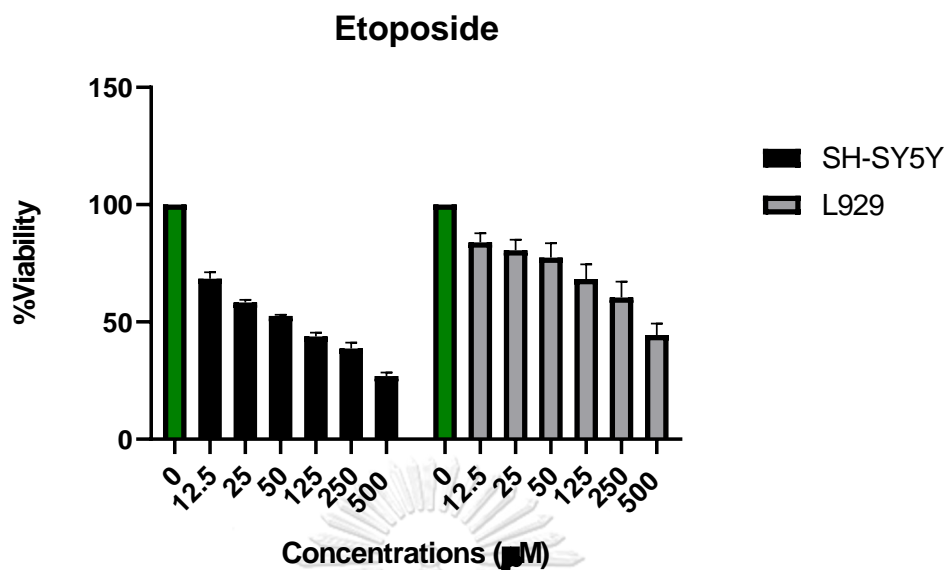


Figure 4.1 Cytotoxicity testing of the standard anticancer drug (Etoposide) in SH-SY5Y and L929 cells. Data are shown as mean \pm SD, n=3.

Figure 4.1 depicts the viability trend observed when testing with etoposide, a standard drug. The results demonstrate a consistent and expected pattern, where increasing concentrations of etoposide lead to a gradual decrease in cell viability. This trend serves as a validation of the assay's sensitivity and ability to accurately measure changes in cell viability in response to cytotoxic compounds.

Further research is needed to explore the specific peptides in riceberry rice and their potential role in antioxidant activity and mitigating ER stress.

4.2 Toxicity of the synthetic peptides derived from riceberry hydrolysates in SH-SY5Y cells

Before proceeding with further experiments, it is essential to assess the potential toxicity of the samples. If the samples prove to be toxic to the cells, it would hinder the progression of subsequent experiments. Therefore, it is crucial to confirm that the peptides derived from riceberry rice exhibit a high percentage of cell viability upon treatment. Ideally, the cell viability should approach 100% to ensure the suitability of the peptides for subsequent tests.

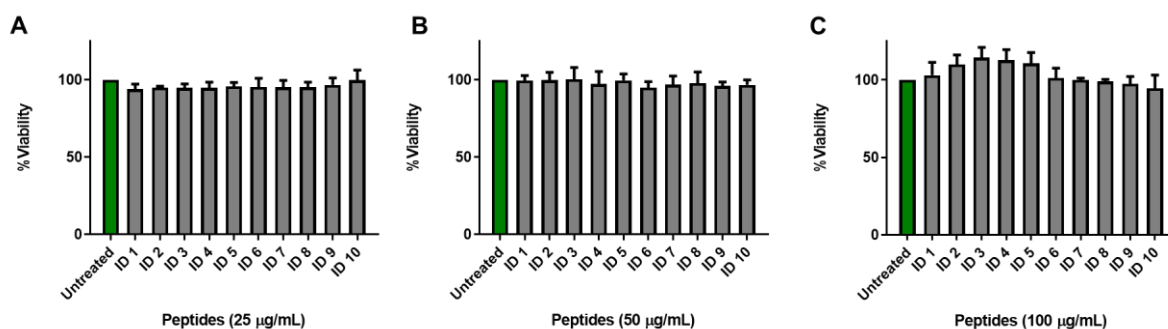


Figure 4.2 Cytotoxicity testing of the A) 25, B) 50, and C) 100 µg/mL peptide hydrolysates from riceberry rice (SH-SY5Y cells). Data are shown as mean \pm SD, n=3

SH-SY5Y cells were exposed to 10 different peptides derived from riceberry rice at concentrations of 25, 50, and 100 µg/mL. The results indicated no signs of cellular toxicity. Notably, the cell viability of cells treated with peptides at a concentration of 25, 50, and 100 µg/mL exceeded 90%, ranging from approximately 93% to more than 100% (Figure 4.2A-C).

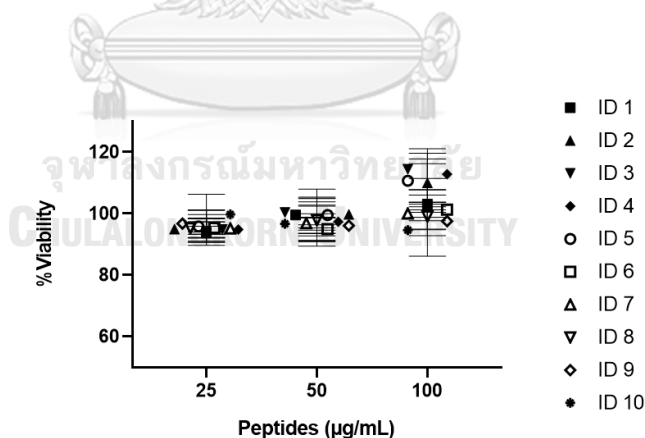


Figure 4.3 The conclusion of the results regarding the toxicity of peptides derived from riceberry rice at concentrations of 25, 50, and 100 µg/mL (SH-SY5Y). Data are shown as mean \pm SD, n=3

Moreover, the viability of cells treated with higher some peptide concentrations appears to be higher compared to lower concentrations (Figure 4.3). This observation

suggests that increasing the peptide concentration may enhance the protective effects against oxidative stress and result in improved cell viability. These findings suggest that the tested peptides derived from riceberry rice are well-tolerated by SH-SY5Y cells and do not exhibit cytotoxic effects within the tested concentration range.

4.3 Determining the appropriate concentration of H₂O₂ and IAA to induce oxidative stress in cells (SH-SY5Y cells)

Hydrogen peroxide (H₂O₂) and iodoacetic acid (IAA) were utilized as oxidative stressors to investigate the antioxidant activity of peptide hydrolysates derived from riceberry rice in cells setting. These stressors were selected based on their ability to induce oxidative stress within cells, creating conditions that allow for the evaluation of the peptides' antioxidant properties. Peptides demonstrating potential antioxidant activity are expected to protect cells from elevated levels of reactive oxygen species (ROS) induced by the oxidative stressors.

Consequently, the cell viability of the peptide-treated groups should exhibit a higher percentage of cell viability compared to the control, which consists of cells treated with the oxidative stressors alone. This is because the oxidative stressors increase the production of ROS, which can lead to cellular apoptosis. As a first step, H₂O₂ at a concentration of 500 μM was used to study oxidative stress in ARPE-19 cells, as described in a relevant research paper²⁵. Therefore, different concentrations of H₂O₂ (500, 1000, and 2000 μM) were applied in cells setting to determine the optimal condition for evaluating the protective effects of peptides on reducing oxidative stress induced by H₂O₂ in SH-SY5Y cells.

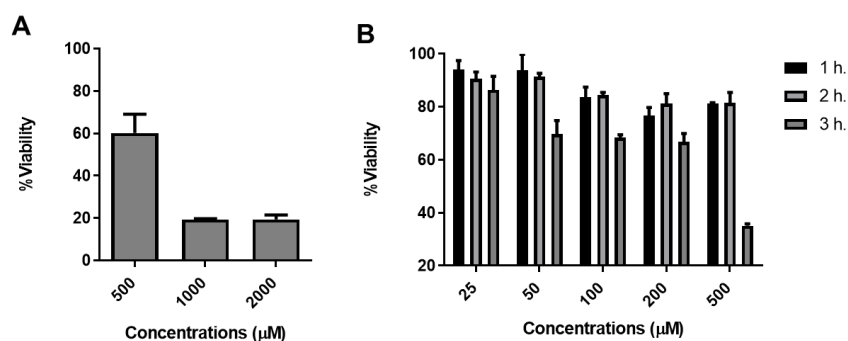


Figure 4.4 Determining the appropriate concentration of A) H₂O₂ and B) IAA to induce oxidative stress in cells (SH-SY5Y cells). Data are shown as mean ± SD, n=3.

The results demonstrated that the cell viability percentages at concentrations of 500, 1000, and 2000 μM of H₂O₂ were found to be approximately 60.2 ± 8.93%, 19.3 ± 0.543%, and 19.4 ± 2.16%, respectively (Figure 4.4A). However, it should be noted that the concentrations of 1000 and 2000 μM caused detachment of the formazan crystals, which are the product of the MTT assay. This detachment could introduce errors in measuring the absorbance in the MTT assay. Therefore, based on these findings, the concentration of 500 μM was selected as the appropriate concentration to assess the antioxidant activity.

The effects of IAA, a chemical known to increase ROS levels, were investigated. Elevated ROS can lead to mitochondrial stress, DNA damage, and oxidative stress in cells²⁴, contributing to the development of various diseases associated with oxidative stress such as cardiovascular diseases⁵² and Alzheimer's disease⁵³. Therefore, this study employed IAA in SH-SY5Y cells to determine the concentrations that induce oxidative stress and subsequent apoptosis.

The cell viability was assessed using the MTT assay after the induction of oxidative stress in the cells. The cells were exposed to various concentrations of IAA (25, 50, 100, 200, and 500 μM), for a duration of 3 h. The evaluation of cell viability revealed that the percentage of viability for cells treated with 200 and 500 μM IAA was approximately 66.8 ± 3.11%, and 35.1 ± 0.719%, respectively (Figure 4.4B).

Based on these results, the concentration of 500 μM will be used to evaluate the protective effects of peptides on oxidative stress induced by IAA in cells. This concentration was chosen because it allows for a clear distinction between the effects of antioxidant activity. If the peptides can protect the cells from the harmful effects of H_2O_2 and IAA and result in higher cell viability compared to the positive control (H_2O_2 and IAA alone), it would indicate their antioxidant activity.



4.4 Assessment of peptide toxicity and evaluation of antioxidant activity in SH-SY5Y cells

Oxidative stress was induced using H₂O₂ and IAA at concentrations of 500 μM for H₂O₂ and 200 and 500 μM for IAA. The antioxidant activity of peptides derived from riceberry rice was assessed using the MTT assay, which determines cell viability. Peptides with antioxidant activity are anticipated to shield cells from oxidative stressors, leading to a higher percentage of cell viability.

In this study, we aimed to investigate the protective effects of peptides against oxidative stress induced by IAA in SH-SY5Y cells. We conducted a comparative analysis by including an IAA alone group treated with IAA at a concentration of 200 or 500 μM for a duration of 3 h. Each experimental set involved peptide treatment in addition to IAA alone.

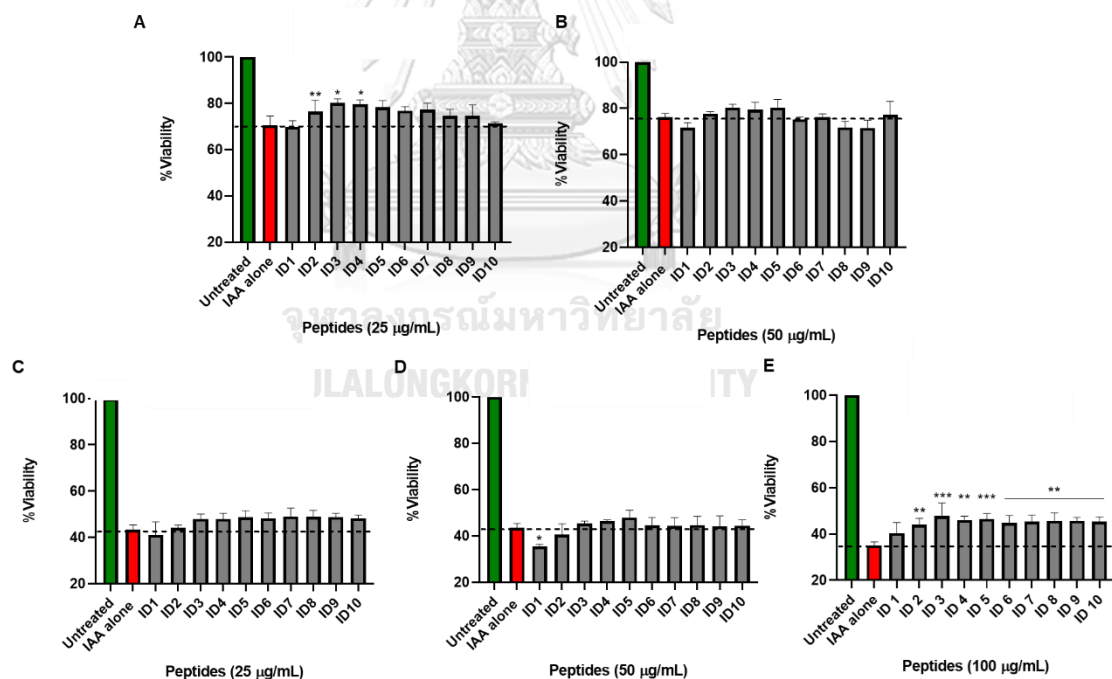


Figure 4.5 Antioxidant activity of riceberry rice peptides at A) 25 B) 50 μg/mL against IAA 200 μM C) 25 D) 50 and E) 100 μg/mL against with IAA 500 μM (SH-SY5Y). Data are shown as mean ± SD, n=3, and (*) denote significant differences compared to IAA alone (p<0.05).

In the experiment, SH-SY5Y cells were treated with peptides at a concentration of 25 $\mu\text{g}/\text{mL}$ for one day and exposed to IAA at a concentration of 200 μM for 3 h. (Figure 4.5A). The results showed that peptide ID 3, ID 4, and ID 5 exhibited significant differences compared to the cells treated with IAA alone. These peptides demonstrated notable protective effects against the oxidative stress induced by IAA. However, when the cells were treated with peptides at a higher concentration of 50 $\mu\text{g}/\text{mL}$ and exposed to IAA (Figure 4.5B), there were no significant differences observed compared to the cells treated with IAA alone. This indicated that both concentrations have similar activity against IAA. These findings highlight the potential of peptide ID 3, ID 4, and ID 5 in mitigating the detrimental effects of oxidative stress induced by IAA in SH-SY5Y cells. Further investigations may be needed to explore the optimal concentrations of peptide treatment for maximum protective effects.

In the subsequent experiment, the concentration of IAA was increased to 500 μM . Cells were treated with peptides at concentrations of 25 $\mu\text{g}/\text{mL}$, 50 $\mu\text{g}/\text{mL}$, and 100 $\mu\text{g}/\text{mL}$. The results showed that at concentrations of 25 $\mu\text{g}/\text{mL}$ (Figure 4.5C) and 50 $\mu\text{g}/\text{mL}$ (Figure 4.5D), none of the peptides exhibited significant higher viability compared to IAA alone. This suggests that at these lower peptide concentrations, none of the peptides were able to provide significant protection against the oxidative stress induced by 500 μM of IAA.

However, when the cells were treated with peptides at a higher concentration of 100 $\mu\text{g}/\text{mL}$ (Figure 4.5E), significant higher viability was observed in the treated peptide group compared to IAA alone. This indicates that at this higher concentration, the peptides demonstrated more pronounced potential protective effects against the oxidative stress induced by IAA. It is important to note that peptide ID 1 showed lower viability compared to the other peptides. This suggests that peptide ID 1 may not effectively protect cells from the oxidative stress induced by IAA. Overall, these findings indicate that the concentration of both the peptides

and IAA can influence the protective effects against oxidative stress in SH-SY5Y cells. Peptides at a concentration of 100 $\mu\text{g}/\text{mL}$ exhibited more notable protective effects, while peptide ID 1 showed a lack of protective efficacy. Further studies are necessary to elucidate the underlying mechanisms and optimize the concentration and treatment duration of the peptides for maximum protective effects.

Although the difference in viability between the peptides at 25 and 50 $\mu\text{g}/\text{mL}$ and IAA alone was not statistically significant, it is still worth noting that peptides ID 3, 4, and 5 consistently demonstrated higher viability compared to other peptides in this concentration group. While the difference may not reach statistical significance, this trend suggests that these peptides may have some protective effects against the oxidative stress induced by IAA. Notably, at a concentration of 100 $\mu\text{g}/\text{mL}$, peptides ID 3, 4, and 5 displayed the highest antioxidant activity, and a significant difference was observed compared to IAA alone. This further supports the idea that these peptides have notable protective effects against oxidative stress.

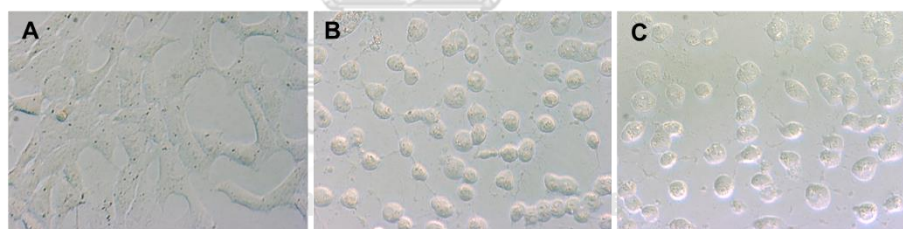


Figure 4.6 Microscopic analysis of SH-SY5Y cellular morphology at 10X magnification A) untreated (healthy cells), B) IAA alone, and C) treated with peptide ID 3 and IAA.

Figure 4.6 displays the cellular morphology of SH-SY5Y cells observed under a 10X magnification microscope. Figure 4.6A represents the untreated group, where cells exhibit a normal and healthy morphology with distinct features. Figure 4.6B depicts cells treated with IAA (500 μM) alone, demonstrating noticeable alterations in cellular morphology, including cell shrinkage, irregular shape, and loss of cellular extensions. These changes reflect the impact of oxidative stress induced by IAA on

cell morphology. Figure 4.6C depicts cells treated with a combination of peptide (50 $\mu\text{g}/\text{mL}$) and IAA (500 μM). Interestingly, the morphology observed in this image appears to be similar to that of cells treated with IAA alone.

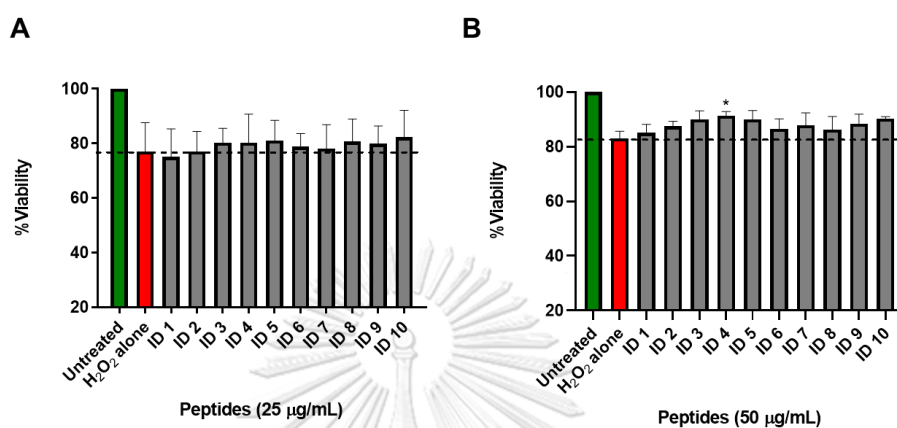


Figure 4.7 Investigating the effectiveness of A) 25 and B) 50 $\mu\text{g}/\text{mL}$ of peptides in mitigating oxidative stress induced by H₂O₂ at a concentration of 500 μM . Data are shown as mean \pm SD, $n=3$, and (*) denote significant differences compared to H₂O₂ alone ($p < 0.05$).

In the subsequent experiment, the oxidative stressor was changed to H₂O₂ at a concentration of 500 μM . Initially, the cells were treated with peptide at a concentration of 25 $\mu\text{g}/\text{mL}$ (Figure 4.7A), but no significant difference was observed compared to H₂O₂ alone. Consequently, the peptide concentration was increased to 50 $\mu\text{g}/\text{mL}$ (Figure 4.7B). Interestingly, only peptide ID 4 exhibited a significant difference in viability compared to H₂O₂ alone, indicating its potential protective effect against H₂O₂-induced oxidative stress.

It is worth noting that the toxicity induced by H₂O₂ was relatively low, as the cell viability remained above 70% in the H₂O₂-treated group. Based on this observation, it was decided not to conduct the peptide treatment at a concentration of 100 $\mu\text{g}/\text{mL}$, as it may not result in a significant improvement in cell viability. Furthermore, although only peptide ID 4 showed a significant difference in viability,

peptides ID 3 and 5 yielded interesting results in terms of cell viability. Although not statistically significant, the trend of higher viability in these peptide-treated groups suggests that they may possess some protective effects against H₂O₂-induced oxidative stress.

4.5 Assessment of peptide toxicity and evaluation of antioxidant activity in L929 cells

The cell model was changed from neuroblastoma cells (SH-SY5Y) to normal cells (L929). This shift in cell type allows for the evaluation of peptide effects on oxidative stress and cell viability in a different cellular context. The experimental setup involved treating L929 cells with oxidative stressors such as IAA or H₂O₂, both alone and in combination with peptides. The viability and protective effects of the peptides on oxidative stress-induced cell damage were assessed and compared to the control groups.

By using L929 cells, which represent a normal cell line, this experiment provides valuable insights into the potential protective effects of the peptides under physiological conditions. It allows for a more comprehensive understanding of the peptides' therapeutic potential in reducing oxidative stress and promoting cell viability in non-cancerous cells.

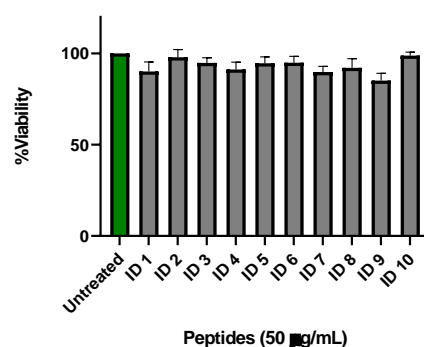


Figure 4.8 Toxicity of the 50 µg/mL peptide hydrolysates from riceberry rice (L929 cells). Data are shown as mean ± SD, n=3.

The concentration of 50 $\mu\text{g/mL}$ was chosen as a representative concentration within the range of 25 to 100 $\mu\text{g/mL}$ to evaluate the toxicity of the peptides derived from riceberry. After treating L929 cells with peptides at a concentration of 50 $\mu\text{g/mL}$ for 24 h., the results (Figure 4.8) indicate that there is no observed toxicity associated with this concentration. Based on the observed lack of toxicity in both L929 and SH-SY5Y cells, it is reasonable to predict that these peptides may also exhibit no toxicity in other cell types. Therefore, they can be utilized for evaluating the antioxidant activity of the peptides.

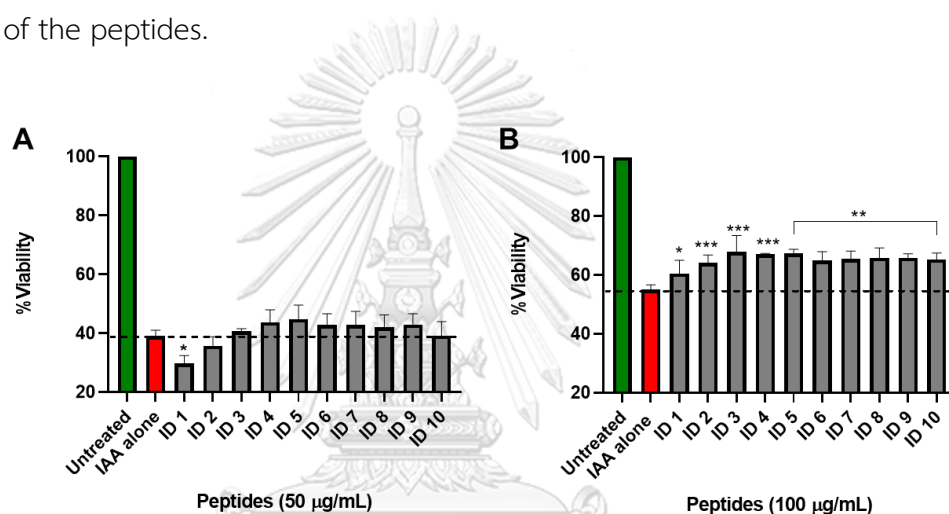


Figure 4.9 Antioxidant activity of riceberry rice peptides at A) 50 and B) 100 $\mu\text{g/mL}$ against IAA 500 μM in L929 cells. Data are shown as mean \pm SD, and (*) denote significant differences compared to IAA alone ($p < 0.05$).

In the experiment using L929 cells, both IAA (500 μM) and H_2O_2 were employed as oxidative stressors. The cells were treated with peptides at concentrations of 50 and 100 $\mu\text{g/mL}$ against with IAA 500 μM illustrated that at the concentration of 50 $\mu\text{g/mL}$ (Figure 4.9A), peptide ID 1 exhibited a significant decrease in viability compared to IAA alone. However, peptides ID 4 and 5, despite not showing a significant difference, displayed the highest viability among the tested peptides. When treated with peptides at a concentration of 100 $\mu\text{g/mL}$ (Figure 4.9B), all peptides demonstrated a significant increase in viability compared to IAA alone. Particularly, peptides ID 3 to 5 exhibited the highest significant differences in viability

when compared to IAA alone. These findings suggest that peptides ID 3 to 5 possess potent protective effects against oxidative stress induced by IAA in L929 cells.

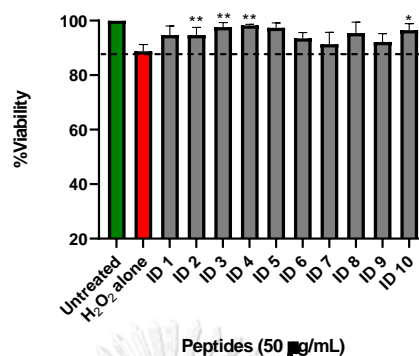


Figure 4.10 Investigating the effectiveness of 50 µg/mL of peptides in mitigating oxidative stress induced by H₂O₂ at a concentration of 500 µM in L929 cells. Data are shown as mean ± SD, and (*) denote significant differences compared to IAA alone (p<0.05).

When L929 cells were treated with peptides at a concentration of 50 µg/mL in the presence of H₂O₂ (500 µM), it was observed that peptides ID 3, ID 4, ID 5, and ID 10 exhibited the highest significant differences in viability compared to cells treated with H₂O₂ alone (Figure 4.10). This suggests that these peptides have strong protective effects against oxidative stress induced by H₂O₂ in L929 cells. The increased viability observed in these peptide-treated groups indicates their potential in mitigating the detrimental effects of H₂O₂ on cell viability.

In summary, the experimental findings obtained from both SH-SY5Y and L929 cells provide important insights regarding the protective effects of peptides against oxidative stress and ER stress. In the case of SH-SY5Y cells treated with 200 µM of IAA, peptide ID 3 to 5 demonstrated significant cell viability and exhibited notable protection compared to the control group. Furthermore, when assessing the protective effects of peptides against oxidative stress induced by 500 µM of IAA at different concentrations (25, 50, and 100 µg/mL), peptide ID 1 displayed lower cell viability, indicating a weaker protective effect. Notably, peptide ID 3 to 5 exhibited the highest cell viability and showed a significant difference compared to the control

group (in case of IAA 500 μM and peptide 100 $\mu\text{g/mL}$). Moreover, peptide ID 4 demonstrated the highest protective effects against 500 μM of H_2O_2 at a concentration of 50 $\mu\text{g/mL}$.

Similar trends were observed in L929 cells, where peptides ID 3 to 5, and 10 showed promising results. Specifically, when tested against IAA at a concentration of 500 μM and different peptide concentrations (50 and 100 $\mu\text{g/mL}$), peptides ID 3 to 5 consistently displayed the highest activity among the tested peptides. In addition, peptide ID 3 to 5, and 10 have the highest protective effects against 500 μM of H_2O_2 at a concentration of 50 $\mu\text{g/mL}$. These findings suggest that peptides ID 3 to 5, and 10 possess strong antioxidant properties and may be effective in protecting cells against ER stress.

Overall, these results highlight the potential of peptides ID 3 to 5, and 10 as candidates for further investigation, as they demonstrate promising characteristics and show potential for mitigating oxidative stress and protecting against ER stress in cells.

4.6 Determining the reduction of ER stress in cells via MTT Assay

For our next experiment, we utilized tunicamycin (TM) as an inducer of ER stress to assess the potential of peptides in reducing ER stress. As ER stress can lead to cell apoptosis, we initially employed the MTT assay to evaluate the impact of peptides on cell viability before proceeding to other assays. In the MTT assay, we treated the cells with TM at a concentration of 20 $\mu\text{g/mL}$. Our hypothesis was similar to previous experiments, suggesting that the groups treated with peptides would exhibit higher percentages of cell viability compared to the control group treated with TM alone.

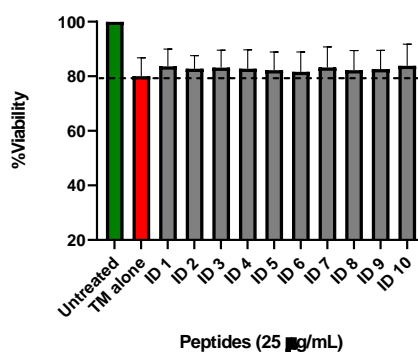


Figure 4.11 The protective effects of riceberry rice peptides on ER stress induced by tunicamycin (TM) 20 µg/mL. Data are shown as mean \pm SD, and (*) denote significant differences compared to TM alone ($p < 0.05$).

The results demonstrated that the viability of cells treated with TM at 20 µg/mL for 24 h. remained high, with approximately 80% viability (Figure 4.11). There were no significant differences observed compared to the peptides-treated group. As a result, the incubation time of TM was extended from 24 h. to 48 h. causes the detachment of the formazan from the plate. Therefore, we attempted to solve this problem by employing a method in which we did not remove the MTT reagent and instead directly added DMSO to dissolve the formazan crystals. However, this approach proved ineffective as the solubility of formazan was significantly reduced when the MTT reagent was not removed.

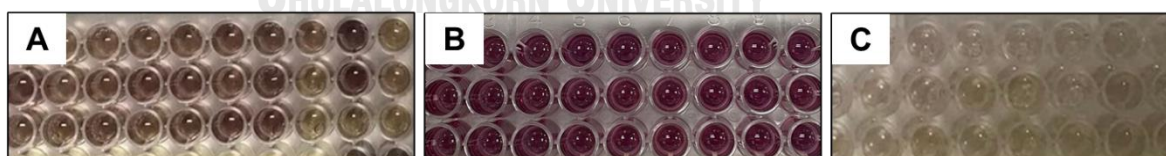


Figure 4.12 The MTT results obtained using different protocols prior to adding

the solvent (DMSO) were compared. A) involved not removing the MTT solution before dissolving it with DMSO, B) removing the MTT solution before dissolving it with DMSO, and C) removing the MTT solution before dissolving it with DMSO specifically in the case of experiments with TM for 48 h.

Figure 4.12A demonstrates the presence of a distinct two-layered solution, with one layer containing formazan crystals and the other layer consisting of DMSO solvent. This contrasts with Figure 4.12B which shows a well-mixed solution obtained through a standard protocol where the medium was removed before adding DMSO to dissolve the formazan. Therefore, in an attempt to prevent the detachment of formazan crystals, we carefully removed the solution while taking precautions to avoid disturbing the formazan. However, despite our efforts, some formazan crystals were still inadvertently removed during the process. As a result, when adding the solvent (DMSO), the resulting solution exhibited a significantly reduced purple color intensity, as depicted in the Figure 4.12C. Therefore, evaluating the potential effect of reducing ER stress via MTT assay may not be suitable in this experiment.

4.7 Characterization of ER stress responses in SH-SY5Y and L929 cells using fluorescence imaging

The cells were stained with concanavalin A (ConA), which is labeled with a green fluorophore, to visualize its localization in the endoplasmic reticulum (ER) and Golgi apparatus. Additionally, DAPI staining (blue fluorophore) was performed to label the cell nuclei.

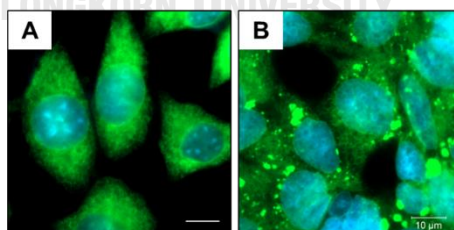


Figure 4.13 Fluorescence images of (A) L929 cells, and (B) SH-SY5Y cells stained with ConA and DAPI.

The morphology of L929 cells (Figure 4.13A) was initially observed as they exhibit a characteristic single-cell morphology, which is easier to visualize compared to SH-SY5Y cells (Figure 4.13B). SH-SY5Y is a neuroblastoma cell line commonly used

to study neurodegenerative disorders. These cells exhibit a neuron-like phenotype²⁸ and have a short proliferation time, allowing for rapid growth²⁹. However, this phenotype poses challenges when observing the cells under a microscope due to difficulties in controlling cell density and isolating individual cells. One of the challenges arises from the rapid proliferation rate, which can result in a higher number of cells within a given timeframe. This can lead to overcrowding, making it difficult to achieve an optimal cell density for microscopic observation. Furthermore, the neuron-like characteristics of SH-SY5Y cells make it challenging to distinguish and isolate individual cells for observation. Neuronal cells have a tendency to form connections and adhere to neighboring cells, complicating the visualization and analysis of single cells.

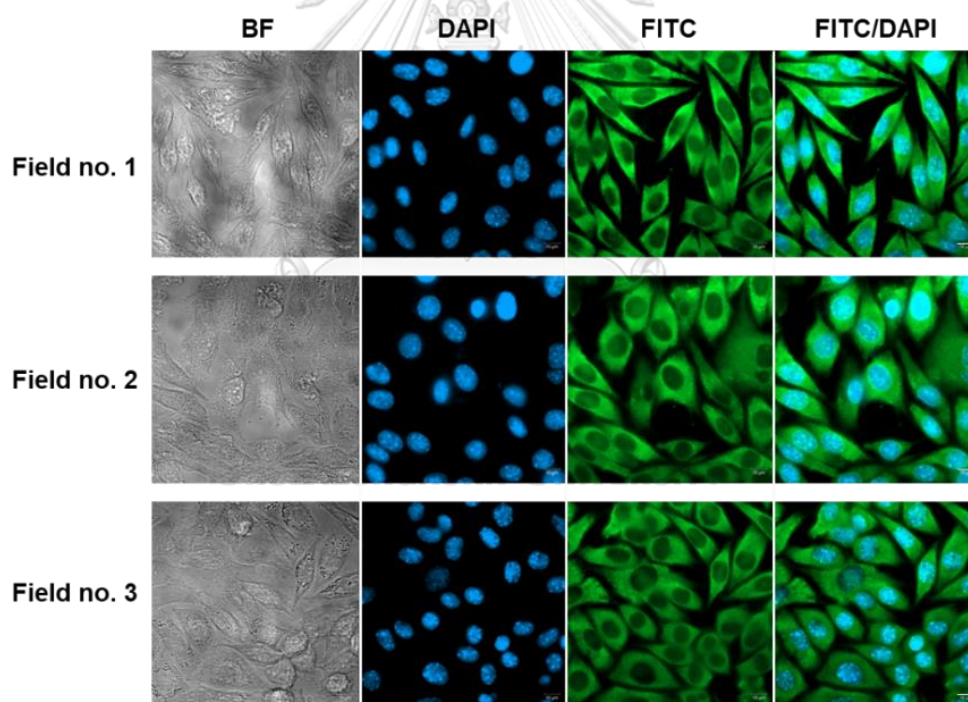


Figure 4.14 Fluorescence images of L929 cells were cultured in a cell culture medium without any treatment of peptides or tunicamycin (TM) stained with DAPI (blue) and ConA (green) by DAPI and FITC channel.

In the initial experiment, L929 cells were treated with peptides derived from riceberry rice for a duration of 24 h. Additionally, the cells were exposed to TM at a

concentration of 10 $\mu\text{g}/\text{mL}$ for a period of 8 h. L929 cells were cultured in a cell culture medium without any treatment of peptides or TM. These cells exhibited the characteristic morphology of fibroblast cells, which is typical for L929 cells. They served as the control group, representing healthy and untreated cells in the experiment (Figure 4.14). The morphology of the untreated group showed that the nuclei (stained blue with DAPI) had a round shape, indicating the typical nuclear morphology. Additionally, the ConA staining mostly exhibited a fibroblast-like shape, reflecting the characteristic morphology of L929 cells.

The morphology of cells treated with TM at a concentration of 10 $\mu\text{g}/\text{mL}$ for 8 h. showed noticeable differences compared to the healthy cell group. The nuclei appeared to have an altered shape and the overall cell morphology appeared to be affected by the TM treatment. These changes suggest that the TM treatment induced morphological alterations in the cells, potentially indicating the presence of ER stress. The treatment with TM at a concentration of 10 $\mu\text{g}/\text{mL}$ for 8 h. resulted in a change in the morphology of L929 cells. Specifically, the cells exhibited a rounder shape, and in some cases, the cells appeared to have transformed into circular shapes. The fading or decreased intensity of DAPI staining in cells can occur when cells undergo toxicity or cell death. This observation is significant as it is often associated with cellular changes that occur prior to apoptosis, suggesting that the TM treatment may be inducing ER stress and lead to cause apoptosis in the L929 cells (Figure 4.15).

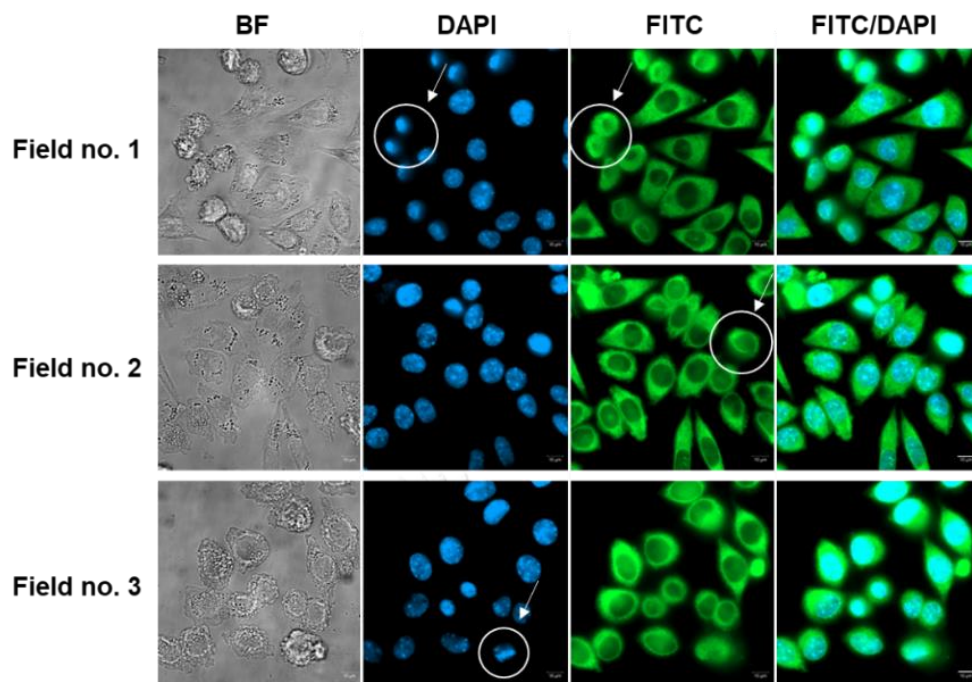


Figure 4.15 Fluorescence images of L929 cells treated with TM for 8 h., an inducer of ER stress.

In the case of peptides that have protective effects in reducing ER stress, it is expected that the morphology of L929 cells should be similar to the untreated group or the control group. This means that the cells treated with the peptides should exhibit a morphology resembling healthy, untreated cells, indicating the potential of the peptides to mitigate ER stress-induced changes in cell morphology. In the treated peptide groups, all peptides demonstrated the ability to protect certain cells from ER stress. The presence of a circular area in the images indicates some examples of a toxic morphology, which could be attributed to the effects of TM or ER stress.

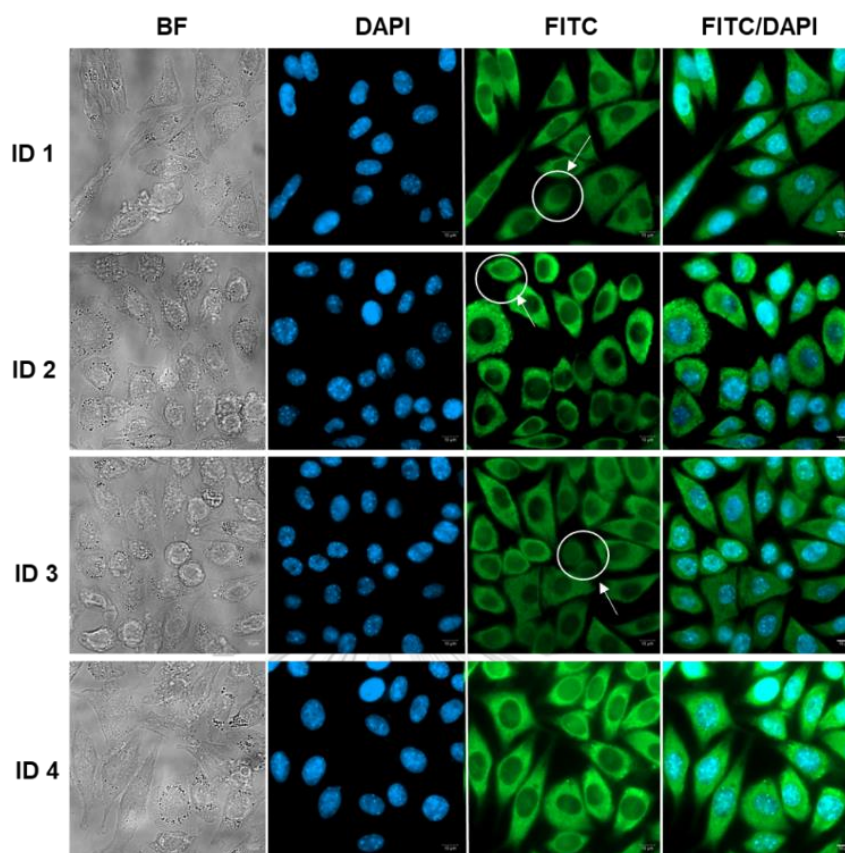


Figure 4.16 Fluorescence images of L929 cells treated with peptides ID 1 to 4 and induced ER stress by TM 10 $\mu\text{g}/\text{mL}$ for 8 h.

However, the treated peptides (Figure 4.16 and Figure 4.17) showed a protective effect on a portion of the cells, suggesting their potential in mitigating the detrimental effects of ER stress and maintaining a healthier cellular morphology compare with cells treated with TM (Figure 4.15). Nevertheless, peptides ID 3 and ID 4 displayed notable protective effects in reducing ER stress, as evidenced by a higher proportion of cells maintaining a preserved and healthy morphology.

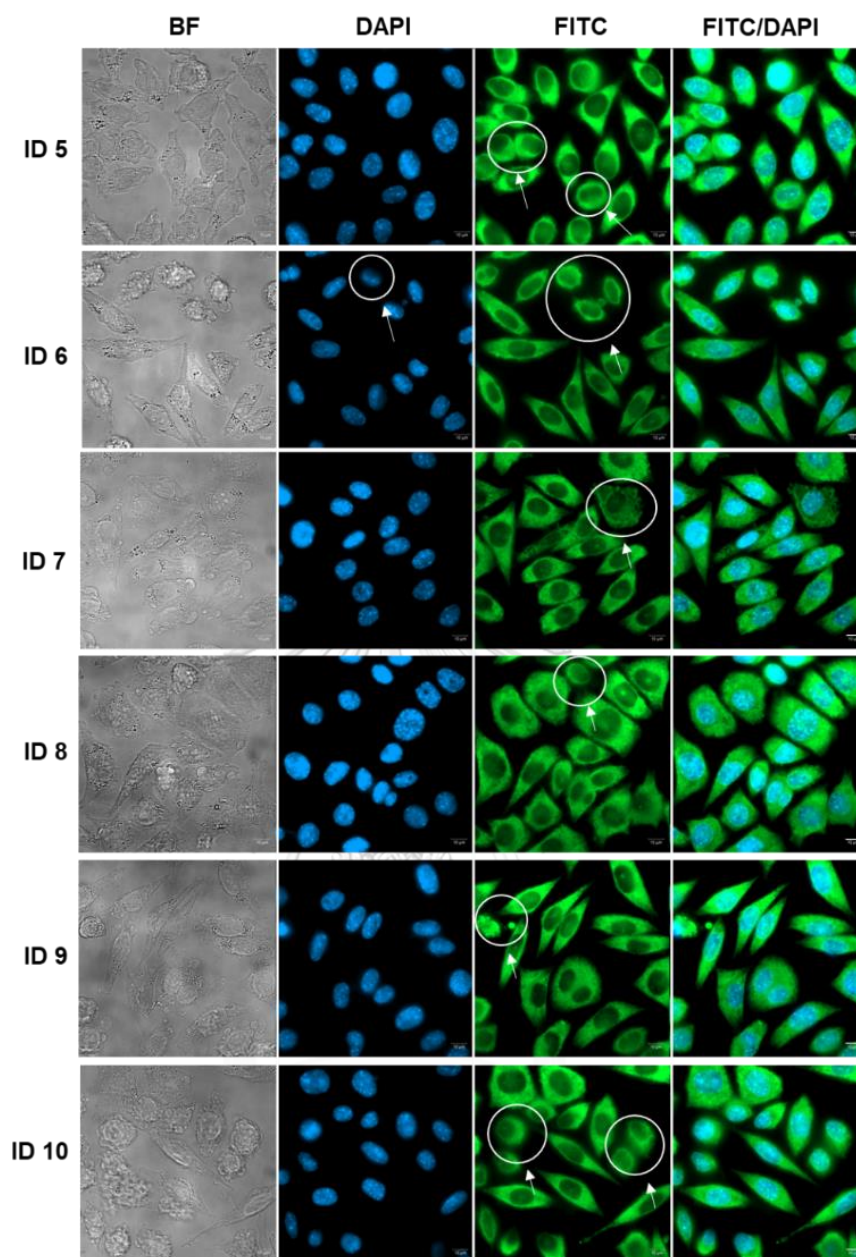


Figure 4.17 Fluorescence images of L929 cells treated with peptides ID 5 to 10 at 50 $\mu\text{g}/\text{mL}$ and induced ER stress by TM 10 $\mu\text{g}/\text{mL}$ for 8 h.

These findings suggest the potential of these peptides in alleviating the detrimental effects of ER stress on cellular structure. However, further experimentation is needed to confirm these hypotheses. Therefore, the time of TM incubation was increased from 8 to 16 h. to gather additional data and validate our observations.

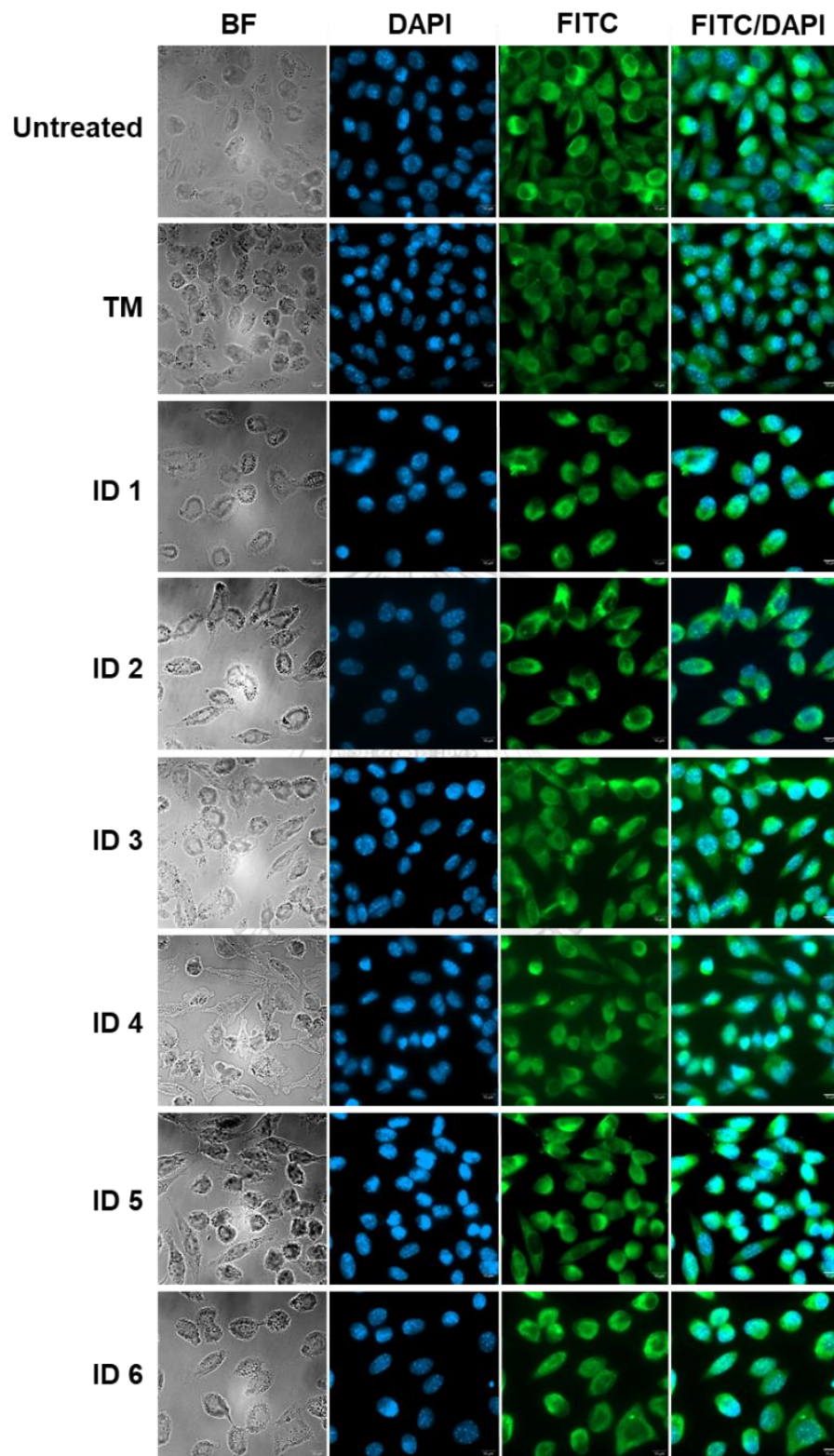


Figure 4.18 Fluorescence images of L929 cells treated with peptides ID 1 to 6 at 50 $\mu\text{g}/\text{mL}$ and induced ER stress by TM 10 $\mu\text{g}/\text{mL}$ for 16 h.

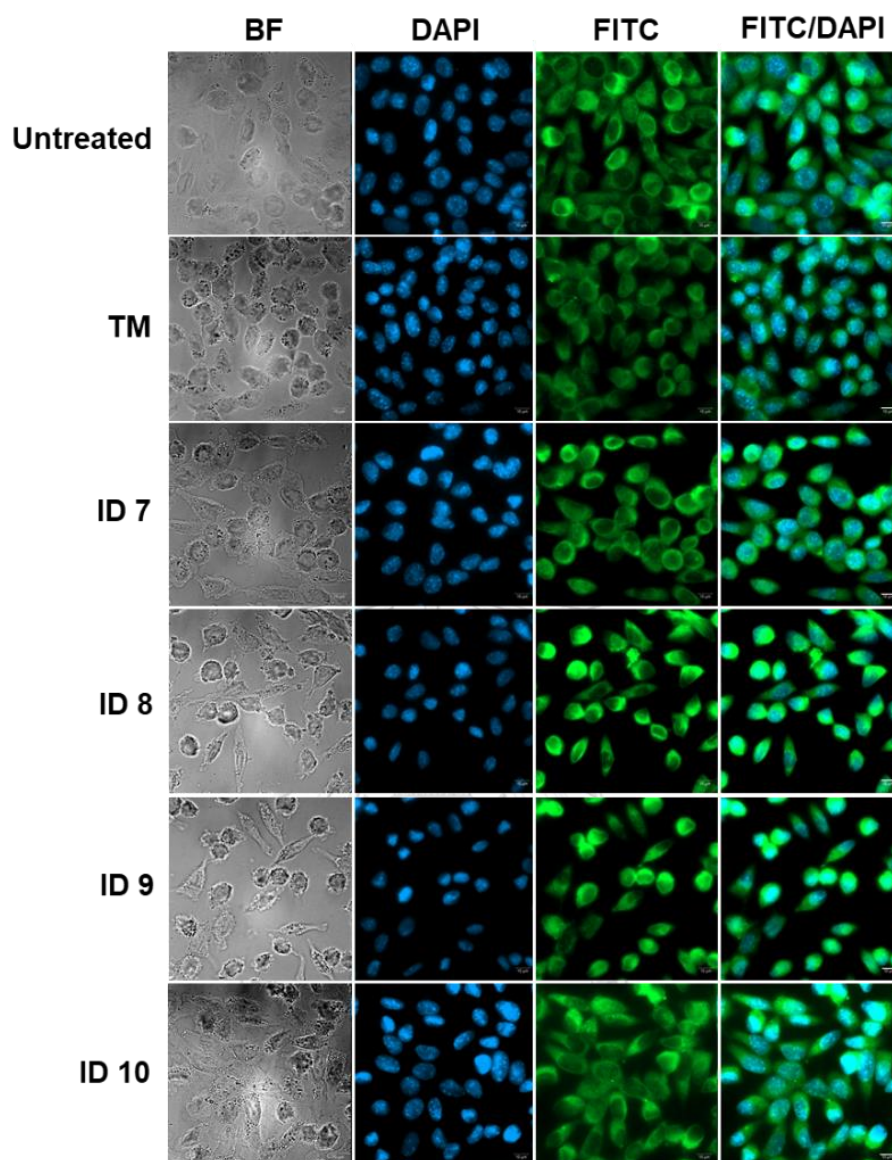


Figure 4.19 Fluorescence images of L929 cells treated with peptides ID 6 to 10 at 50 $\mu\text{g}/\text{mL}$ and induced ER stress by TM 10 $\mu\text{g}/\text{mL}$ for 16 h.

After increasing the incubation time of TM (Figure 4.18 and Figure 4.19), there was an observed increase in the number of cells displaying a circular shape compared to the 8 h. incubation period (Figure 4.16 and Figure 4.17). This change in cell morphology suggests a greater induction of ER stress. Based on these results, we can now screen and identify peptides that have the potential to effectively reduce ER stress and mitigate the circular cell morphology associated with it.

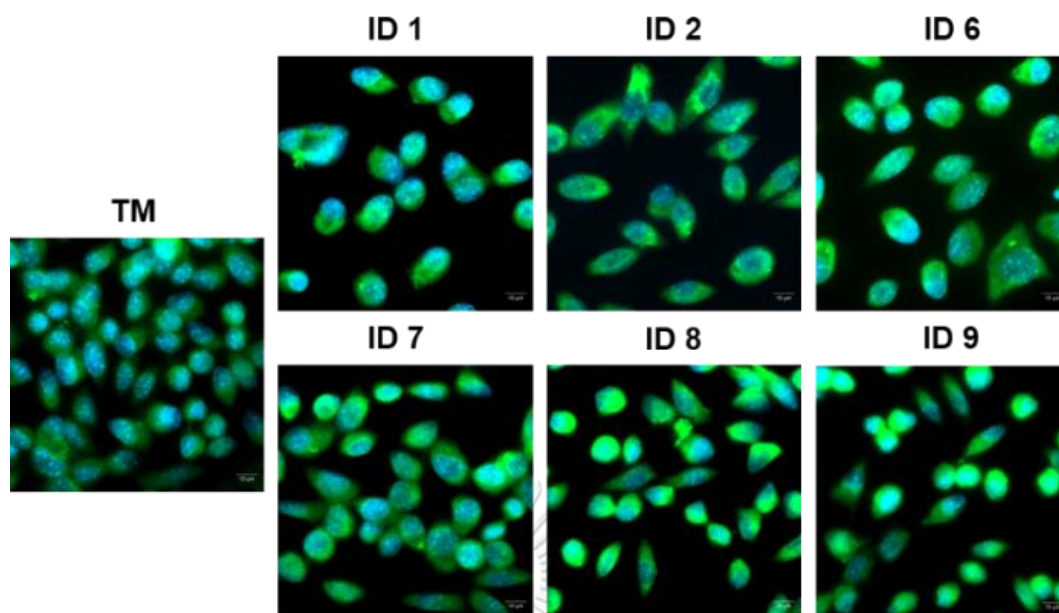


Figure 4.20 Morphological analysis of L929 cells treated with peptides exhibiting the worst morphology.

Peptides ID 3, 4, 5, and 10 exhibited a higher proportion of healthy cells compared to other peptides, suggesting their potential in reducing ER stress. In contrast, peptides ID 1, 2, 6, 7, 8, and 9 showed a lower proportion of healthy cells, indicating their limited effectiveness in reducing ER stress (Figure 4.20). In addition to the toxic morphology observed in cells, peptides with poor protective effects also resulted in a decrease in cell population. This decrease in cell number can be attributed to the detachment of cells from the plates, which is indicative of apoptosis induction. Therefore, peptides that demonstrate lower protective effects not only exhibit toxic morphology but also lead to a reduced cell count due to apoptosis. These findings provide valuable insights into the differential effects of peptides on ER stress reduction.

In the next step, we plan to further increase the incubation time from 16 h. to 24 h. and implement a cropping technique to observe individual cells and compare their morphology. By extending the incubation time, we aim to capture any potential changes in cell morphology and assess the effects of the peptides on

cellular structure. The cropping technique will allow us to focus on specific regions of interest and obtain a more detailed analysis of cell morphology at the single-cell level. In this particular experiment, our focus will be on examining the effects of peptide ID 3, 4, 5, and 10. These peptides have shown promising results in previous experiments regarding their potential to reduce ER stress and protect cells. By specifically studying these peptides, we aim to gain further insights into their mechanisms of action and evaluate their effectiveness in mitigating ER stress-induced cellular changes. The results obtained from this experiment will contribute to our understanding of these peptides' therapeutic potential and their suitability for future applications in addressing ER stress-related conditions.



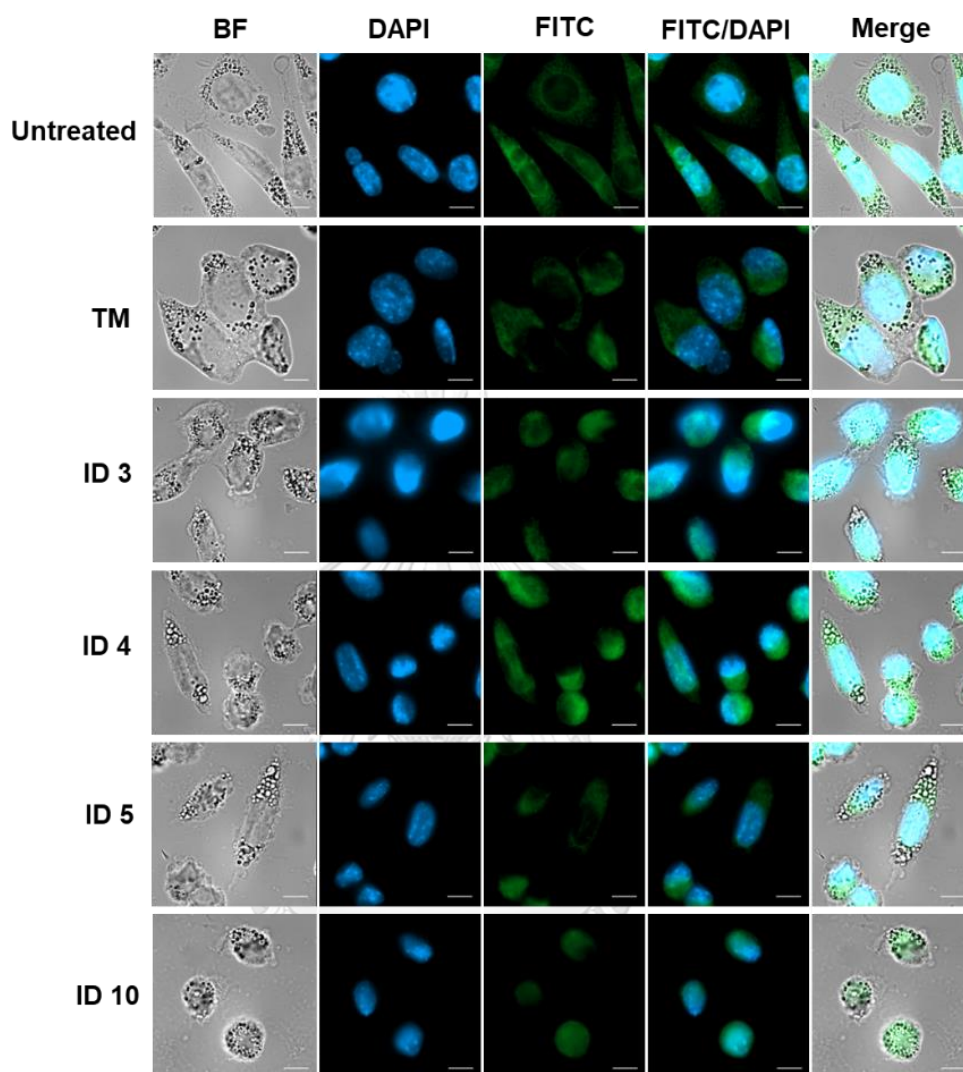


Figure 4.21 Morphological analysis and CTCF measurement of L929 cells of peptides ID 3 to 10 at 50 $\mu\text{g}/\text{mL}$ induced by TM 10 $\mu\text{g}/\text{mL}$ for 24 h. A) morphology of L929 cells stained with ConA (FITC channel) and DAPI under fluorescence microscopy (100X magnification).

Figure 4.21 illustrates a comparison of cellular morphology between untreated L929 cells and those treated with TM. However, it is observed that the fluorescence intensity of the dye appears to be significantly faded compared to

other experiments. This could be attributed to several factors, such as prolonged exposure to the dye, photobleaching, or variations in the experimental conditions.

While the fluorescence intensity of the dye may have faded in Figure 4.21, we will make an effort to analyze and interpret the results to the best of our abilities. Despite the limitations imposed by the faded dye, we can still observe preliminary conclusions based on the available data. Except for peptide ID 10, which showed a distinct pattern, the other peptides (ID 3, 4, and 5) exhibited a fibroblast-like cellular morphology similar to the untreated group. This suggests that these peptides may have protective effects on the ER or Golgi areas, as indicated by the presence of residual fluorescence signal. However, it is important to acknowledge the potential impact of the faded dye on the accuracy and reliability of the results. Further experiments with optimized staining protocols and improved dye stability will be conducted to obtain more conclusive findings in the future. The observation of cell morphology is challenging, particularly when comparing the effects of peptide treatment or TM treatment. Interestingly, the treated cells exhibit similar morphology to the TM-treated group. However, the key difference between the untreated and TM-treated groups lies in the intensity of ConA binding.

TM is known to inhibit N-linked glycosylation and disrupt protein folding processes within the endoplasmic reticulum (ER)⁴⁴. This leads to the accumulation of misfolded proteins within the cells. ConA, a lectin that specifically binds to glycoproteins^{54, 55}, exhibits a higher intensity of binding in the TM-treated group compared to the untreated group. Additionally, an increase in the incubation time of TM from 16 h. to 24 h. results in a higher occurrence of ER stress in cells. This extended incubation time can contribute to variations in the intensity observed between the TM-treated and untreated groups (Figure 4.22A).

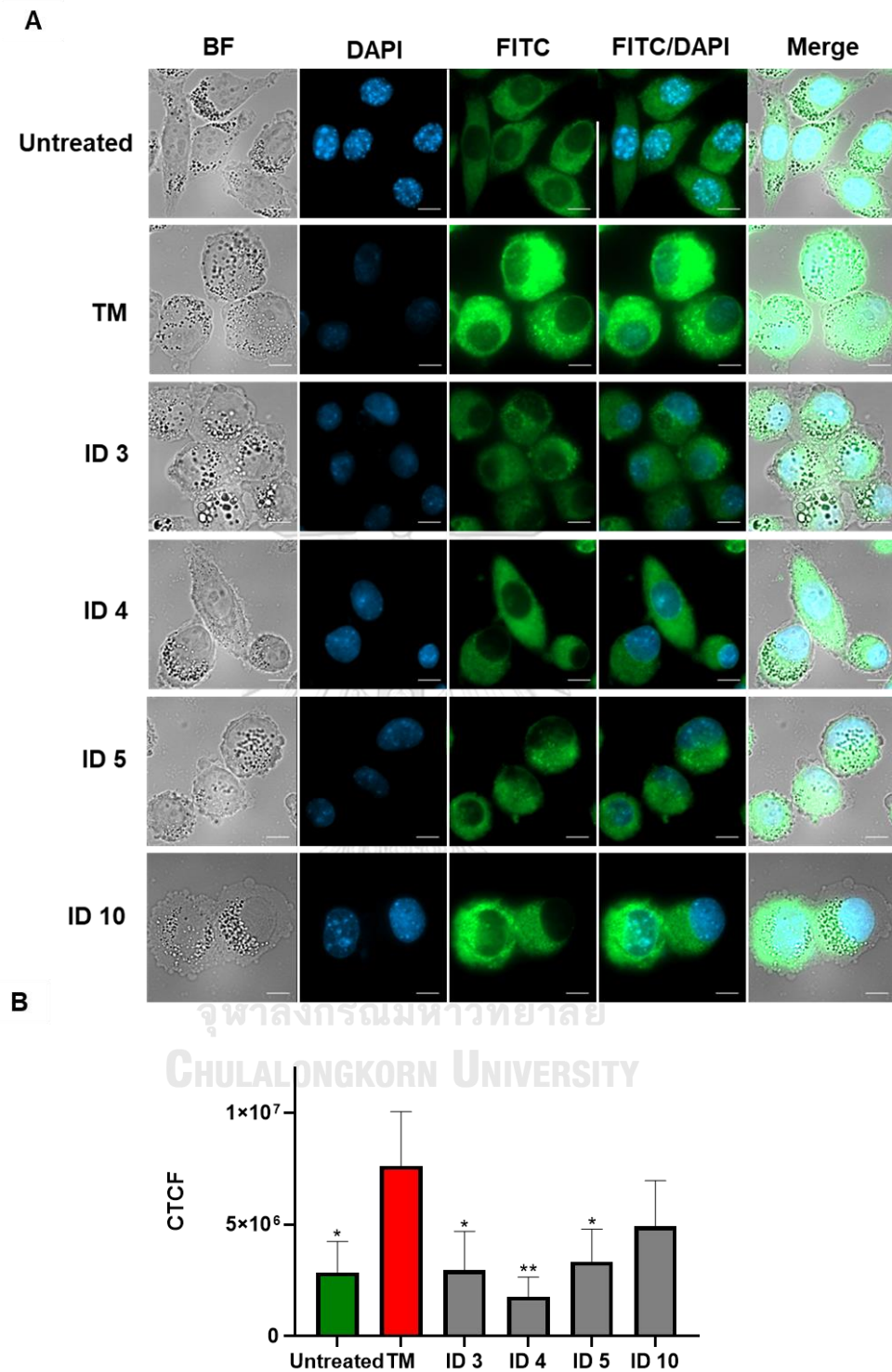


Figure 4.22 Morphological analysis and CTCF measurement of L929 cells treated with peptides ID 3 to 10 at concentrations 50 $\mu\text{g}/\text{mL}$ induced by TM 10 $\mu\text{g}/\text{mL}$ for 24 h. A) morphology of L929 cells stained with ConA (FITC channel) and DAPI under

fluorescence microscopy (100X magnification). B) CTCF measurement of ConA intensity in L929 cells ($p < 0.05$).

CTCF (Corrected Total Cell Fluorescence) is a measurement technique used in ImageJ to quantify cell fluorescence. It calculates the intensity of fluorescence for each individual cell. Higher CTCF values indicate a higher intensity of fluorescence within the cell⁵¹. The group treated with TM alone exhibited the highest CTCF value, indicating a higher ConA intensity of fluorescence. On the other hand, the peptides that have a potential effect on reducing ER stress are expected to show lower CTCF values compared to the TM alone group. However, the analysis revealed that, with the exception of ID 10, all of the groups treated with peptides showed significantly higher CTCF values compared to the TM alone group (Figure 4.22). As a result, peptide ID 10 showed no potential in protecting the cells from TM-induced ER stress. However, further experiments are needed to confirm the potential protective effects of the remaining peptides. In the next step, the concentration of peptides was increased from 50 to 100 $\mu\text{g/mL}$ to investigate whether the protective effects on reducing ER stress are similar to those observed in the previous experiment. This additional experiment will help to further assure the results obtained from the analysis of CTCF in this study.

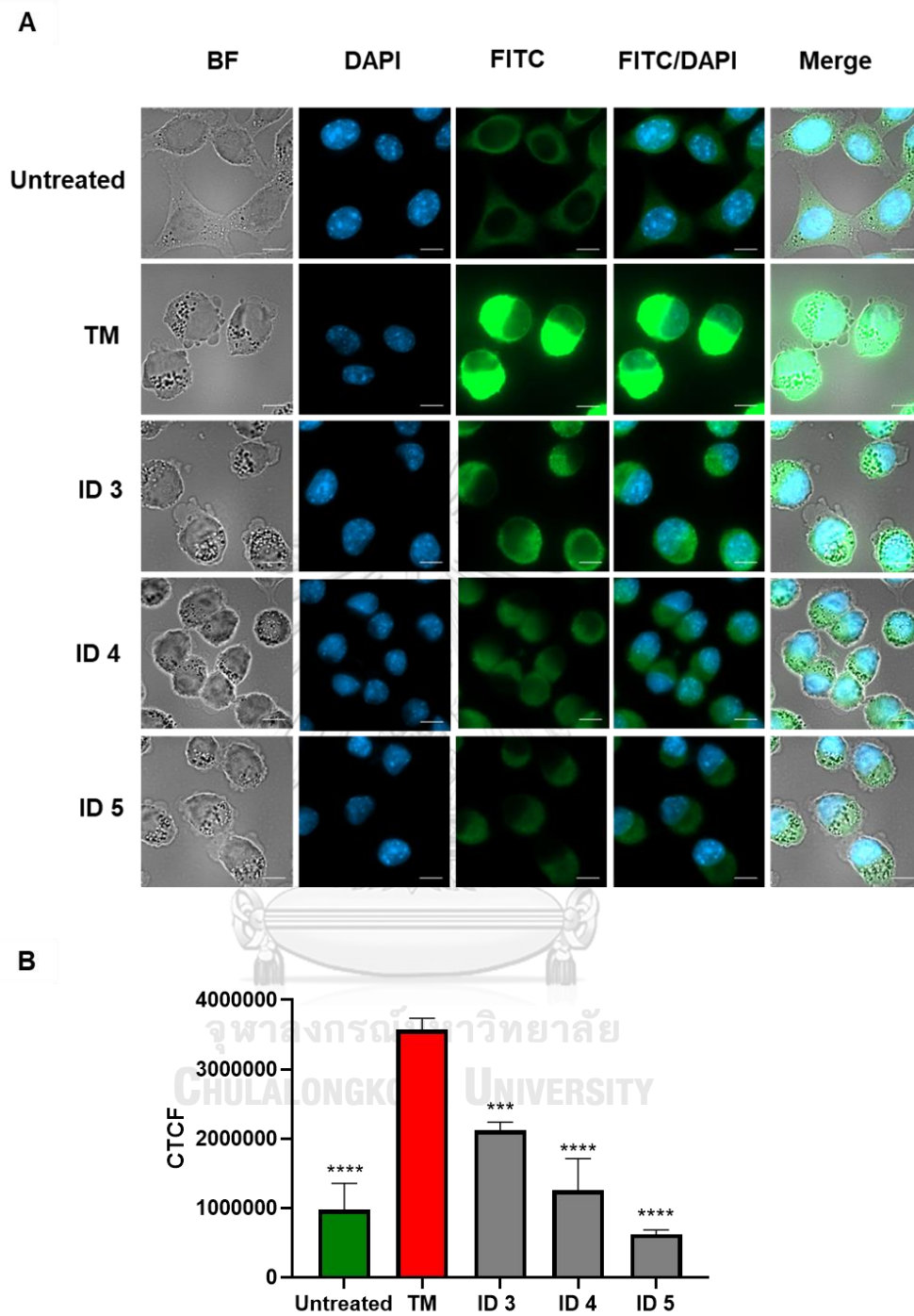


Figure 4.23 Morphological analysis and CTCF measurement of L929 cells treated with peptides ID 3 to 5 at concentrations 100 $\mu\text{g}/\text{mL}$. A) morphology of L929 cells stained with ConA (FITC channel) and DAPI under fluorescence microscopy (100X magnification). B) CTCF measurement of ConA intensity in L929 cells ($p < 0.05$).

After increasing the concentration of peptides (100 $\mu\text{g}/\text{mL}$), a similar trend was observed as seen with the peptides treated at 50 $\mu\text{g}/\text{mL}$. The treatment with peptides ID 3 to 5 showed a significant difference compared to the TM group. All of these peptides exhibited a lower CTCF compared to TM, indicating their potential in reducing ER stress (Figure 4.23). However, the trend observed for each peptide differed from the previous study. At a concentration of 50 $\mu\text{g}/\text{mL}$, the CTCF of ID 4 was lower than that of ID 5. Conversely, at a concentration of 100 $\mu\text{g}/\text{mL}$, ID 5 showed a higher CTCF compared to ID 4. The observed differences in CTCF between peptides at different concentrations could be due to their varying affinities for specific cellular targets involved in the ER stress response. Each peptide may interact differently with these targets, leading to variations in their ability to alleviate ER stress and subsequently affect the fluorescence intensity measured by CTCF. While the specific reason for the contrasting results between ID 4 and ID 5 at different concentrations requires further investigation, it is important to note that the focus of this research is on comparing the peptides' ability to reduce ER stress compared to TM.

Therefore, despite the variations observed between ID 4 and ID 5 at different concentrations, the primary objective of this study is to evaluate the peptides' effectiveness in reducing ER stress relative to the TM group. The differences in CTCF between peptides and TM provide valuable insights into their potential as protective agents against ER stress. Further studies can be conducted to delve into the underlying mechanisms and address the specific differences observed between ID 4 and ID 5 at different concentrations.

Subsequently, the study extended to investigate the protective effects of reducing ER stress in SH-SY5Y neuroblastoma cells using fluorescence imaging techniques. In the experiment involving SH-SY5Y cells stained with ConA, the focus was primarily on analyzing ConA intensity. Previous studies conducted on L929 cells only examined the intensity of ConA staining. Therefore, in this study with SH-SY5Y

cells, the emphasis was placed on presenting the results using the FITC channel, which represents the cells stained with ConA. Additionally, the FITC images were merged with DAPI staining to visualize the nuclei and provide a comprehensive understanding of the cellular morphology and ConA localization within the cells.

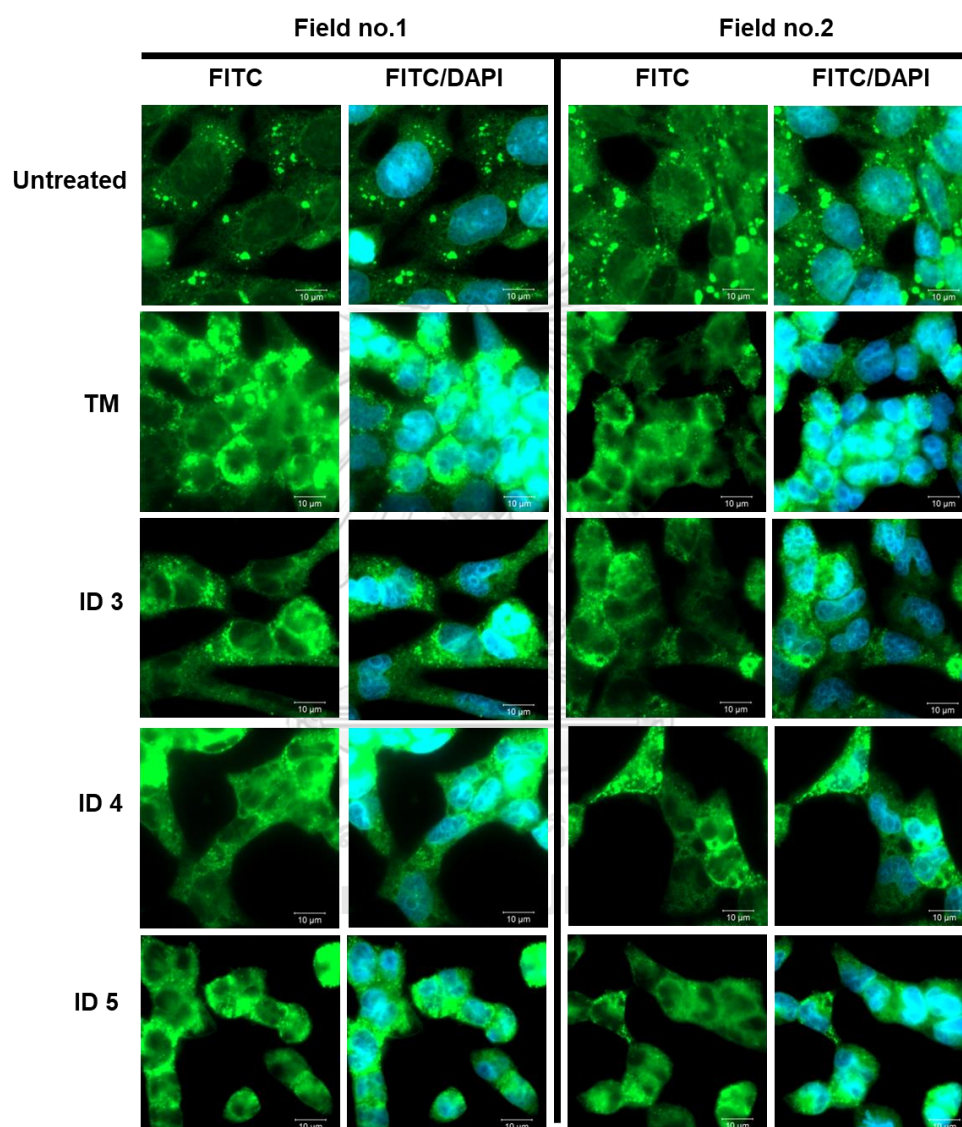
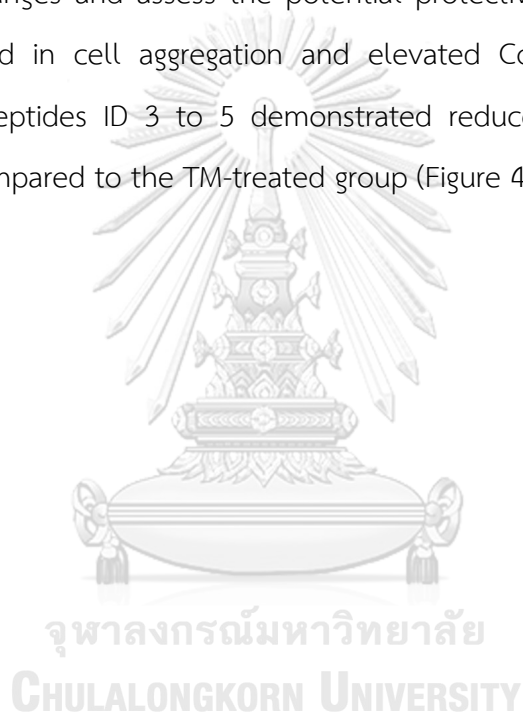


Figure 4.24 Morphological analysis and CTCF measurement of SH-SY5Y cells treated with peptides ID 3 to 5 at concentrations 50 $\mu\text{g}/\text{mL}$ A) morphology of SH-SY5Y cells stained with ConA (FITC channel) and DAPI under fluorescence microscopy (100X magnification). B) CTCF measurement of ConA intensity in SH-SY5Y cells.

The fluorescence images of SH-SY5Y cells stained with ConA and DAPI revealed significant alterations following treatment with TM. The administration of TM led to the formation of cell aggregates and disrupted the clear demarcation of individual cells. Consequently, this posed challenges in accurately measuring CTCF, which is typically assessed on a per-cell basis. The presence of cell aggregates hindered the ability to define distinct cellular boundaries and precisely quantify the fluorescence intensity. Despite these difficulties, it was still possible to observe the morphological changes and assess the potential protective effects. Treatment with TM alone resulted in cell aggregation and elevated ConA intensity. Conversely, treatment with peptides ID 3 to 5 demonstrated reduced aggregation and lower ConA intensity compared to the TM-treated group (Figure 4.24).



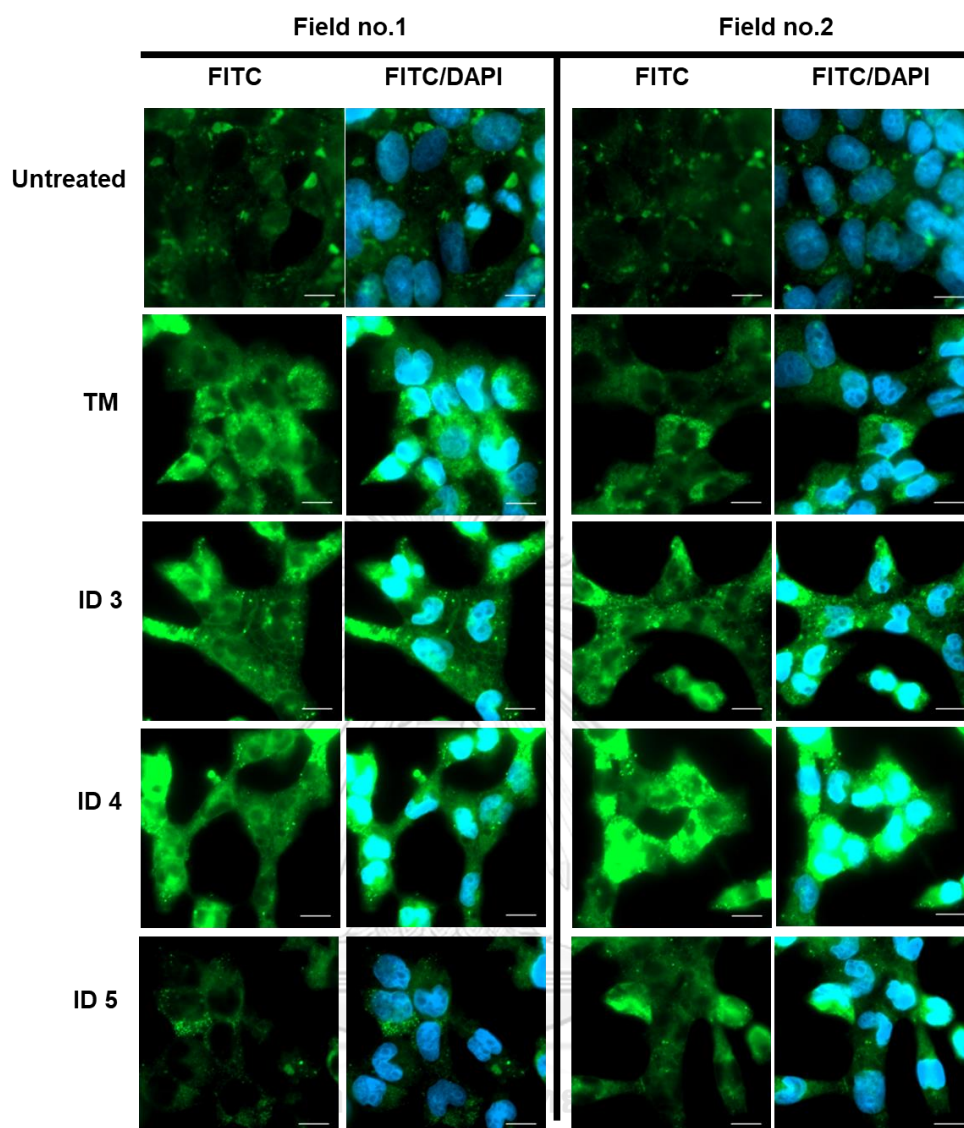


Figure 4.25 Morphological analysis and CTCF measurement of SH-SY5Y cells treated with peptides ID 3 to 5 at concentrations 100 $\mu\text{g}/\text{mL}$ A) morphology of SH-SY5Y cells stained with ConA (FITC channel) and DAPI under fluorescence microscopy (100X magnification). B) CTCF measurement of ConA intensity in SH-SY5Y cells.

Figure 4.25 reveal two distinct effects following TM treatment in SH-SY5Y cells. Firstly, cell aggregation, as observed in the previous experiment, was observed. Secondly, in some fields, a significant reduction in ConA staining intensity was observed.

The cell aggregation observed suggests that TM treatment induces cellular stress, potentially impacting cellular structures and interactions. This aggregation may be associated with an increased accumulation of misfolded proteins, leading to higher ConA staining intensity, indicative of glycoproteins associated with ER stress. During the UPR, cells undergo adaptive mechanisms to restore ER homeostasis. This includes upregulation of chaperone proteins, such as GRP78⁵⁶, which can bind to misfolded proteins and prevent their aggregation leading to the lower intensity of ConA. However, under prolonged or severe ER stress conditions, the capacity of the chaperone system may become overwhelmed, leading to the accumulation of misfolded proteins and high intensity of ConA. Furthermore, individual cellular responses to TM-induced ER stress can vary, resulting in heterogeneous levels of protein misfolding and glycosylation. This can contribute to the variability in ConA staining intensity observed among the treated.

The results obtained from L929 and SH-SY5Y cells demonstrated contrasting patterns in response to TM treatment. In L929 cells, a consistent trend was observed across most fields, where TM treatment resulted in higher intensity of ConA staining. This indicates an increase in glycoproteins associated with ER stress. On the other hand, SH-SY5Y cells exhibited two distinct cases. In some fields, similar to L929 cells, TM treatment led to an increase in ConA staining intensity, suggesting an elevation in ER stress and glycoprotein accumulation. However, in other fields, a different observation was made, with lower ConA staining intensity. This suggests that a subset of SH-SY5Y cells may respond differently to TM-induced ER stress, resulting in reduced glycoprotein accumulation or altered cellular responses.

The challenges in analyzing the results of SH-SY5Y cells, particularly with regards to the high variability in ConA staining intensity following tunicamycin treatment, make it difficult to establish consistent criteria for comparing the effects of peptides and tunicamycin treatment. The presence of two distinct cases, where

some fields exhibit increased ConA intensity while others show lower intensity, adds further complexity to the interpretation of results.

To address this issue, it may be necessary to explore alternative parameters or additional assays that can provide a more reliable and consistent measure of ER stress reduction. This could involve investigating other markers of ER stress, such as the expression levels of specific ER stress-related genes or the activation status of key signaling pathways. By incorporating multiple readouts, a more comprehensive understanding of the effects of peptides compared to TM treatment can be obtained, mitigating the limitations posed by the variability in ConA staining intensity in SH-SY5Y cells.

Indeed, while the variability in ConA staining intensity in SH-SY5Y cells poses challenges in directly comparing the effects of peptides and TM treatment, the results from L929 cells can still be utilized to identify potentially effective peptides.

Based on these findings, it is clear that Figure 4.25 alone cannot definitively determine which peptides have protective effects in reducing ER stress. For a more comprehensive evaluation, it may be more suitable to rely on the imaging results from L929 cells, which can provide insights into potential peptides with protective effects against ER stress in SH-SY5Y cells.

In the case of L929 cells, the consistent pattern of increased ConA intensity following TM treatment provides a reliable baseline for comparison. By examining the effects of peptides on reducing ER stress in L929 cells and comparing their ConA intensities to the TM-treated group, it is possible to identify peptides that exhibit a significant reduction in ConA intensity. These peptides may have the potential to alleviate ER stress in L929 cells.

4.8 Detecting ER Stress by assessing calcium ion (Ca^{2+}) Levels in the endoplasmic reticulum

This experiment aimed to validate our findings involves measuring the intensity of Ca^{2+} in the endoplasmic reticulum (ER) using Mag-fluo4 AM. Mag-Fluo4, a calcium-sensitive fluorescent dye, was employed to assess the level of Ca^{2+} in the endoplasmic reticulum (ER). Decreased Ca^{2+} levels in the ER are indicative of ER stress, a condition characterized by disrupted calcium homeostasis²¹. By utilizing Mag-Fluo4, we can investigate the potential impact of peptides 3, 4, and 5 on mitigating ER stress-induced calcium depletion, shedding light on their ability to regulate Ca^{2+} dynamics and alleviate ER stress.

Both TM and thapsigargin are known to disrupt the homeostasis of Ca^{2+} in the endoplasmic reticulum (ER)²¹. They interfere with the normal functioning of the ER and can lead to an imbalance in the levels of Ca^{2+} , causing ER stress. If peptides have the potential effects on reducing ER stress, we would expect them to exhibit higher intensity of Mag-Fluo4 compared to the group treated with TM.

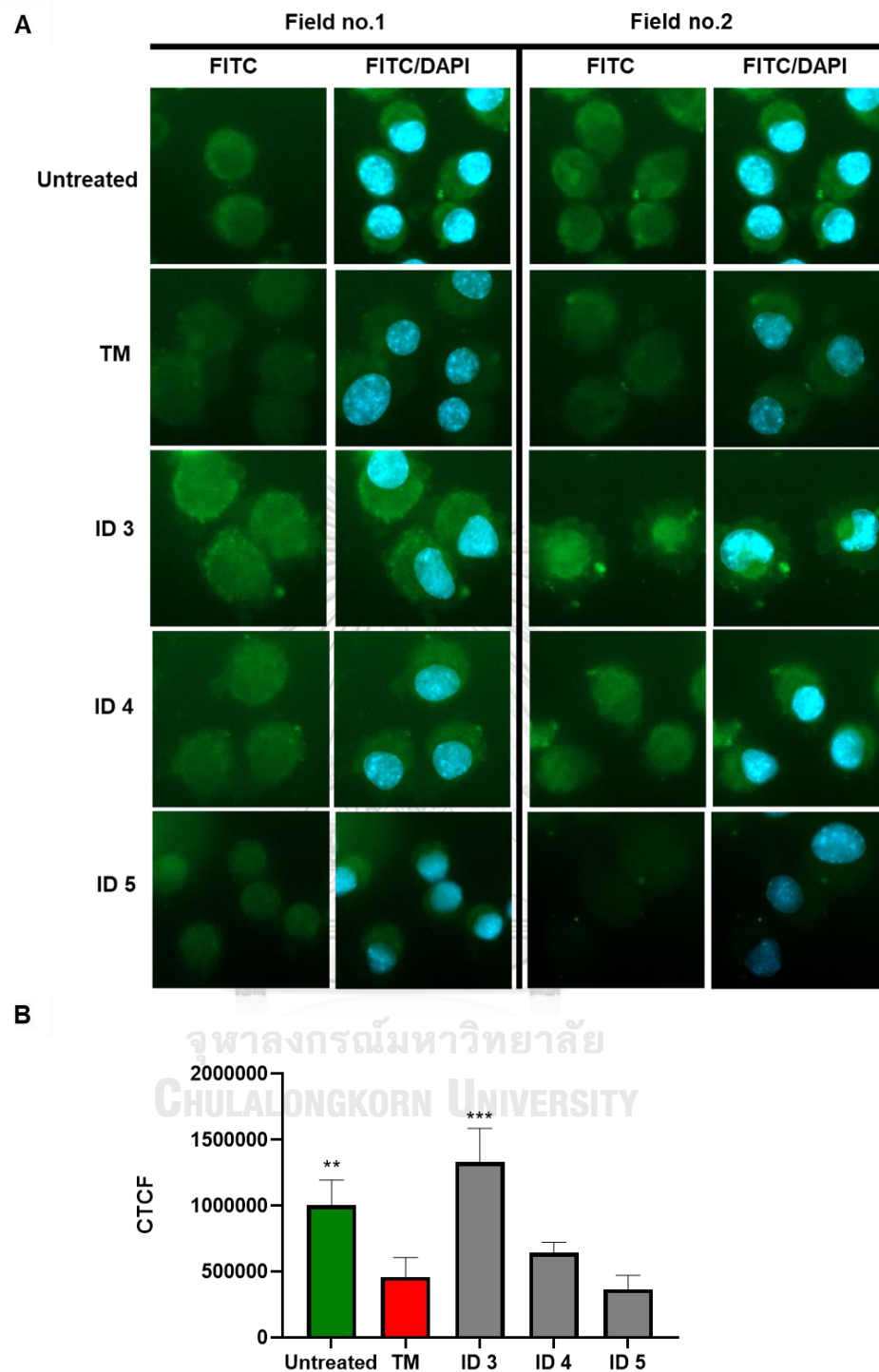


Figure 4.26 Quantification of ER stress-induced Ca^{2+} dysregulation using Mag-Fluo4 and CTCF analysis for assessing the protective effects of peptides ID 3 to 5 at 50 $\mu\text{g}/\text{mL}$ of L929 cells induced by TM 10 $\mu\text{g}/\text{mL}$ for 24 h. A) Fluorescence microscopic

imaging of ER stress at 100X magnification with FITC and DAPI channels B) CTCF from Mag-Fluo4 intensity ($p < 0.05$).

The results of the CTCF analysis indicate that peptide ID 3 exhibited the highest CTCF value, which was significantly higher than that of the TM group (Figure 4.26). These findings suggest that peptide ID 3 has the potential to protect cells from ER stress induced by a decrease in calcium levels. The higher CTCF value suggests a stronger protective effect of peptide ID 3 compared to TM.



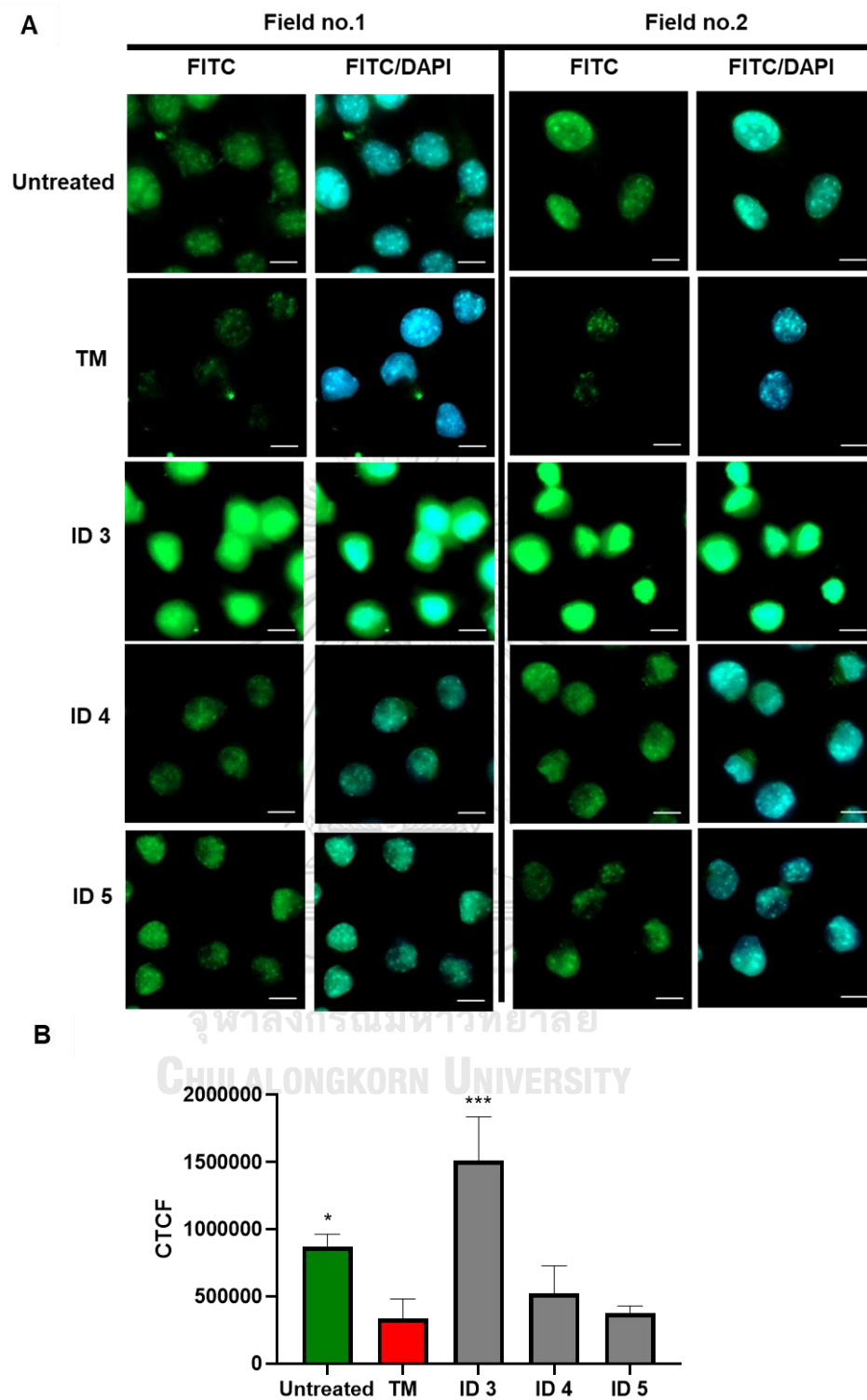


Figure 4.27 Quantification of ER stress-induced Ca^{2+} dysregulation using Mag-Fluo4 and CTCF analysis for assessing the protective effects of peptides ID 3 to 5 at 100 $\mu\text{g}/\text{mL}$ of L929 cells induced by TM 10 $\mu\text{g}/\text{mL}$ for 24 h. A) Fluorescence microscopic

imaging of ER stress at 100X magnification with FITC and DAPI channels B) CTCF from Mag-Fluo4 intensity ($p < 0.05$).

This observation is consistent with the hypothesis that certain peptides can mitigate ER stress by modulating Ca^{2+} levels. The ability of peptide ID 3 to maintain higher CTCF levels suggests its effectiveness in preventing or reducing ER stress-related cellular damage. To validate the findings obtained from the CTCF analysis of Mag-Fluo4 at a peptide concentration of 50 $\mu\text{g/mL}$, we conducted further experiments by increasing the peptide concentration to 100 $\mu\text{g/mL}$. The objective of this supplementary analysis was to verify the observed CTCF values of Mag-Fluo4 at various concentrations of peptides and compare them with the CTCF values of ConA in the TM group. This comprehensive evaluation aimed to confirm the peptide's efficacy in mitigating ER stress and provide a thorough understanding of its potential in reducing ER stress. The trend observed for peptides at a concentration of 100 $\mu\text{g/mL}$ (Figure 4.27) was consistent with the findings at 50 $\mu\text{g/mL}$, indicating that peptide ID 3 consistently exhibited the highest CTCF value when assessed using Mag-Fluo4. However, the obtained results (Figure 4.27) were unexpected, as the areas stained with Mag-Fluo4 appeared to be the same as the areas stained for the nucleus. Ideally, Mag-Fluo4 should selectively stain the endoplasmic reticulum (ER) rather than the nucleus. This error indicates the need for further improvement in the results, particularly for the treatment with peptides at a concentration of 100 $\mu\text{g/mL}$. One possible explanation for these errors could be attributed to the passage number of the cells. As cells undergo multiple passages, they tend to become older, which makes them more susceptible to stress. Consequently, this increased cellular stress could lead to the disappearance or alteration of the ER structure, resulting in the observed similarity between the areas of the nucleus and ER staining. By focusing on the results obtained at this concentration (100 $\mu\text{g/mL}$), we still can confirm the trends and effects observed in the ER stress reduction. It is crucial to acknowledge

that improvements are necessary to ensure accurate and reliable visualization of the ER staining in the future experiments.



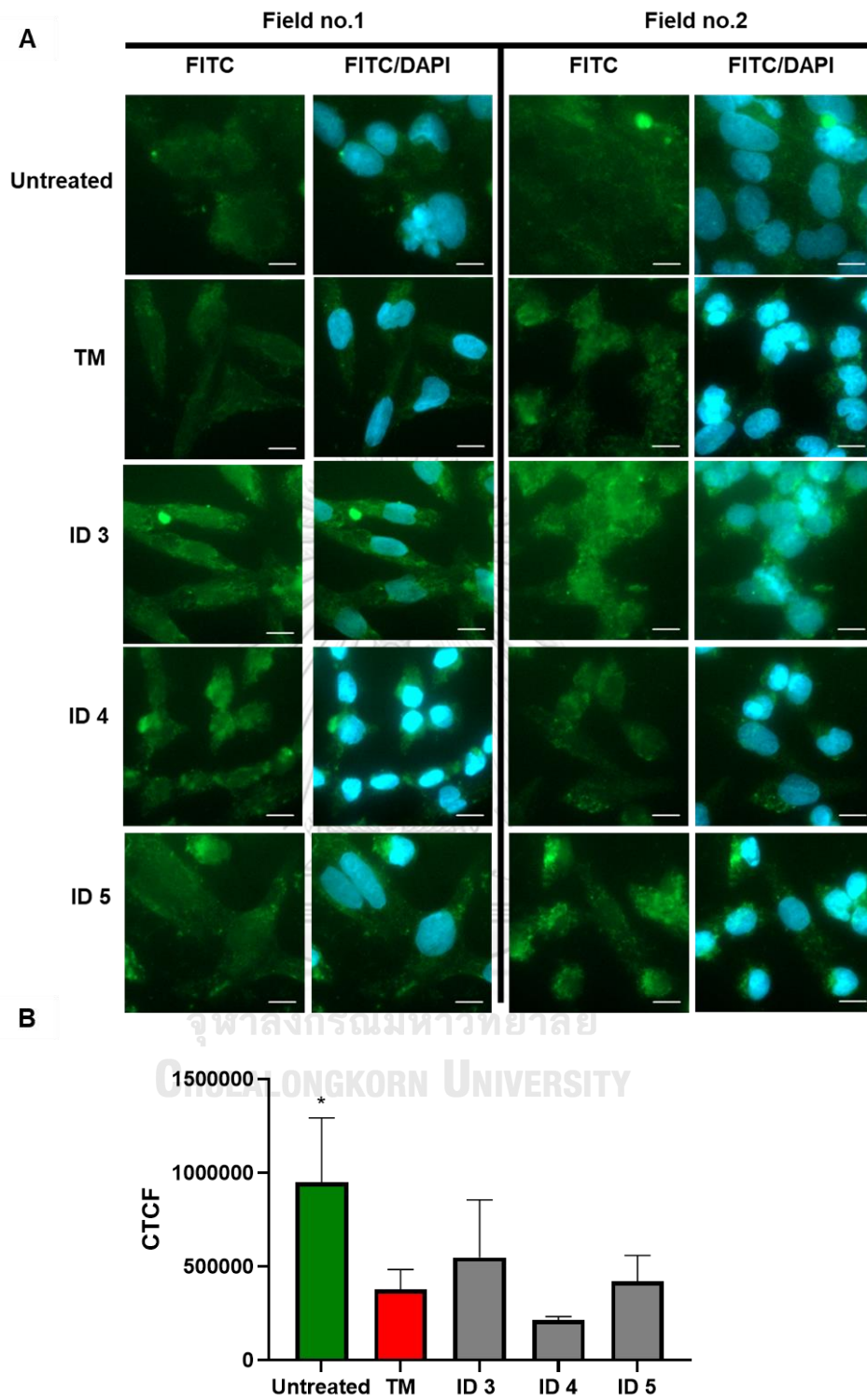


Figure 4.28 Quantification of ER stress-induced Ca^{2+} dysregulation using Mag-Fluo4 and CTCF analysis for assessing the protective effects of peptides ID 3 to 5 at 50 $\mu\text{g}/\text{mL}$ of SH-SY5Y cells induced by TM 10 $\mu\text{g}/\text{mL}$ for 24 h. A) Fluorescence

microscopic imaging of ER stress at 100X magnification with FITC and DAPI channels
B) CTCF from Mag-Fluo4 intensity ($p < 0.05$).

For the SH-SY5Y cells, although it was challenging to identify clear cellular boundaries, we proceeded with measuring the CTCF of Mag-Fluo4. The results showed that peptide ID 3 had the highest CTCF, but it did not show a significant difference compared to the TM group. Similarly, peptide ID 4 and 5 also did not demonstrate a significant difference in CTCF compared to the TM group (Figure 4.28).



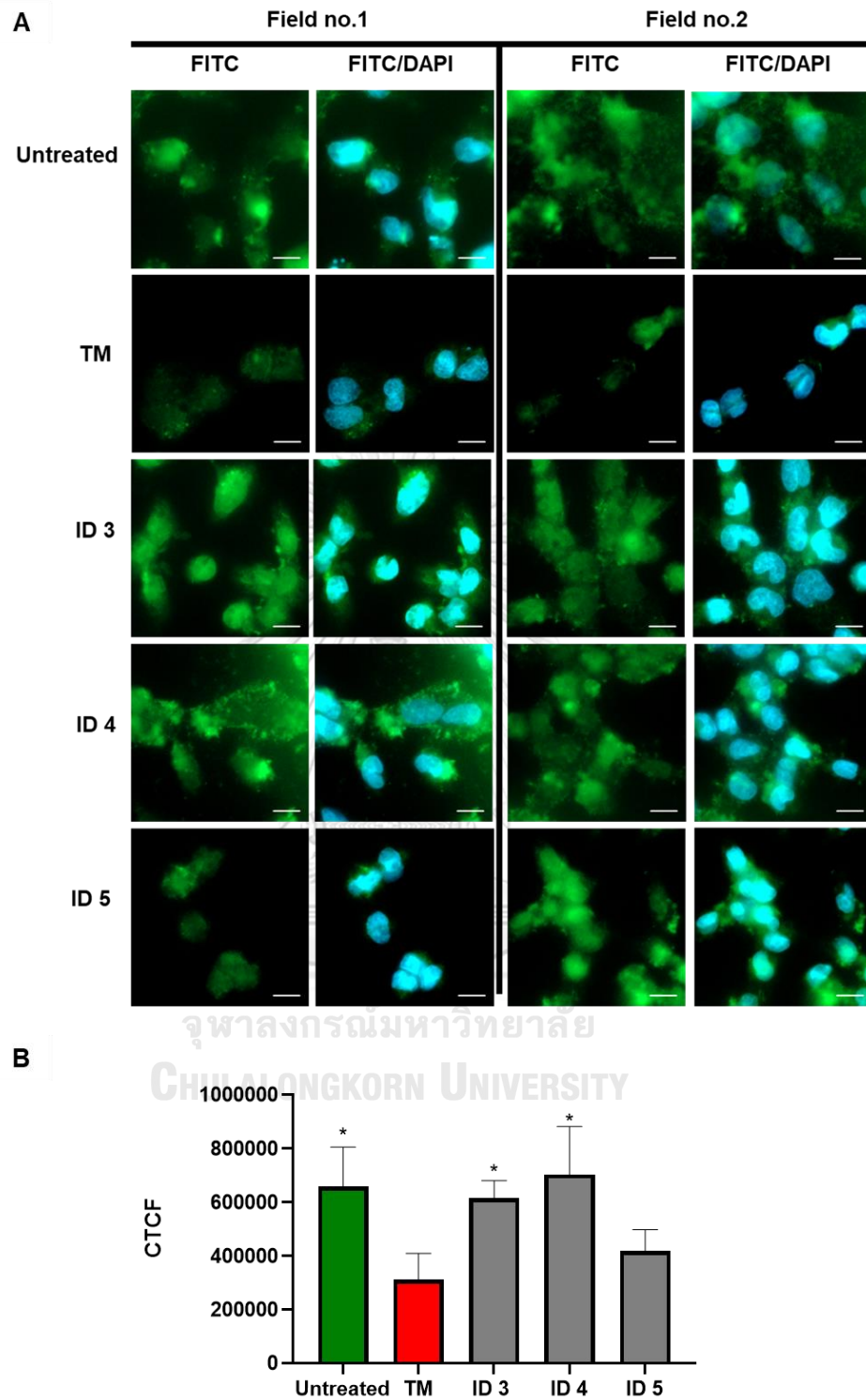


Figure 4.29 Quantification of ER stress-induced Ca^{2+} dysregulation using Mag-Fluo4 and CTCF analysis for assessing the protective effects of peptides ID 3 to 5 at 100 $\mu\text{g}/\text{mL}$ of SH-SY5Y cells induced by TM 10 $\mu\text{g}/\text{mL}$ for 24 h. A) Fluorescence

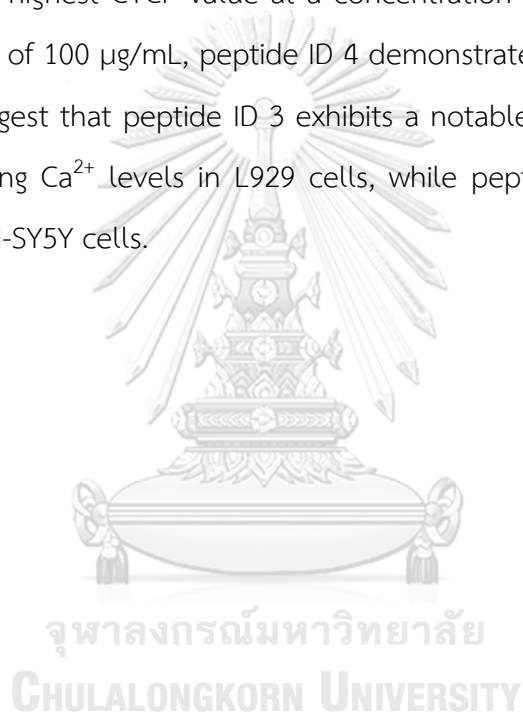
microscopic imaging of ER stress at 100X magnification with FITC and DAPI channels
 B) CTCF from Mag-Fluo4 intensity ($p < 0.05$).

Increasing the concentration of peptides from 50 $\mu\text{g/mL}$ to 100 $\mu\text{g/mL}$ resulted in interesting effects. Specifically, in the case of L929 cells treated with 50 $\mu\text{g/mL}$ and 100 $\mu\text{g/mL}$ of peptide ID 3, the CTCF values were the highest, indicating significant protective effects on reducing ER stress by controlling calcium ion levels. Similarly, in SH-SY5Y cells treated with 50 $\mu\text{g/mL}$ of peptide ID 3, the CTCF values were also the highest, but there was no significant difference compared to the TM group. However, for SH-SY5Y cells treated with 100 $\mu\text{g/mL}$ of peptides, peptide ID 4 demonstrated the highest CTCF value (Figure 4.29). This suggests that SH-SY5Y treated with peptide at a concentration of 100 $\mu\text{g/mL}$, peptide ID 4 may enhance the protective effects associated with reducing ER stress. Further investigations are needed to explore the precise mechanisms underlying these concentration-dependent effects and to determine the optimal concentrations for maximizing the protective effects of both peptide ID 3 and ID 4.

Table 4 Comparative analysis of peptide effects on ER stress reduction: Descending order of CTCF in L929 and SH-SY5Y cells at different peptide concentrations. (*) denote significant differences compared to TM ($p < 0.05$).

Cell Type	Concentration of peptide ($\mu\text{g/mL}$)	Descending orders of CTCF
L929	50	ID 3 [*] > ID 4 > ID 5
	100	ID 3 [*] > ID 4 > ID 5
SH-SY5Y	50	ID 3 > ID 5 > ID 4
	100	ID 4 [*] > ID 3 [*] > ID 5

In conclusion, the assessment of Ca^{2+} levels in L929 and SH-SY5Y cells revealed interesting findings. In L929 cells, treatment with peptides ID 3 to 5 at concentrations of 50 and 100 $\mu\text{g}/\text{mL}$ for 24 h., followed by treatment with TM (10 $\mu\text{g}/\text{mL}$) for an additional 24 h., demonstrated that peptide ID 3, at both concentrations, exhibited the highest CTCF values. This indicates a significant protective effect in reducing ER stress by regulating Ca^{2+} levels within the ER. On the other hand, in SH-SY5Y cells subjected to the same experimental protocol, peptide ID 3 exhibited the highest CTCF value at a concentration of 50 $\mu\text{g}/\text{mL}$. Interestingly, at a concentration of 100 $\mu\text{g}/\text{mL}$, peptide ID 4 demonstrated the highest CTCF value. These findings suggest that peptide ID 3 exhibits a notable potential for reducing ER stress by controlling Ca^{2+} levels in L929 cells, while peptide ID 4 shows promising effectiveness in SH-SY5Y cells.



CHAPTER 5

CONCLUSION

This research investigated the potential effects of riceberry rice peptide hydrolysates on reducing endoplasmic reticulum (ER) stress. Peptides ID 3, 4, 5, and 10 exhibited significant antioxidant activity, protecting cells from oxidative stress induced by iodoacetic acid (IAA) and hydrogen peroxide (H₂O₂). Furthermore, peptide ID 3 to 5 demonstrated the most promising results in reducing ER stress, as indicated by the decreased intensity of the ER-localized dye, ConA and ID 3 and 4 showed the increased intensity of Mag-Fluo4, which is the dye stained the calcium ion (Ca²⁺) levels of ER, compared to the tunicamycin (TM) treatment. These findings suggest that peptide ID 3 and 4 may play a crucial role in regulating ER stress by controlling calcium ion levels. The statistical analysis using one-way ANOVA confirmed the significant differences in ConA intensity between peptide-treated and TM-treated cells (p<0.05). These results highlight the potential of riceberry rice peptide hydrolysates, particularly peptide ID 3 and 4, as valuable dietary supplements for promoting health and well-being by reducing oxidative stress and alleviating ER stress. However, it is important to acknowledge some limitations of this study, such as the use of cell models and the need for further investigation in vivo.

Future research should focus on elucidating the underlying molecular mechanisms of peptide ID 3 and 4 in regulating ER stress, such as through the utilization of techniques like Western blot analysis to examine the expression levels of ER stress markers. Additionally, conducting animal studies and clinical trials would provide valuable insights into the efficacy and safety of these peptide hydrolysates in human subjects, further validating their potential therapeutic applications in mitigating ER stress-related diseases. These comprehensive investigations would

strengthen our understanding of the antioxidant and ER stress-reducing properties of riceberry rice peptides and pave the way for future advancements in this field.



REFERENCES

- (1) Settapramote, N.; Laokuldilok, T.; Boonyawan, D.; Utama-ang, N. Physiochemical, Antioxidant Activities and Anthocyanin of Riceberry Rice from Different Locations in Thailand. *Int. Food Res. J.* **2018**, *6*, 84.
- (2) Chen, A. C.-H.; Burr, L.; McGuckin, M. A. Oxidative and endoplasmic reticulum stress in respiratory disease. *Clin. Transl. Immunol.* **2018**, *7*, e1019.
- (3) Bravo, R.; Parra, V.; Gatica, D.; Rodriguez, A. E.; Torrealba, N.; Paredes, F.; Wang, Z. V.; Zorzano, A.; Hill, J. A.; Jaimovich, E.; et al. Endoplasmic reticulum and the unfolded protein response: dynamics and metabolic integration. *Int. Rev. Cell. Mol. Biol.* **2013**, *301*, 215.
- (4) Jonathan H. Lin, P. W., T.S. Benedict Yen. Endoplasmic Reticulum Stress in Disease Pathogenesis. *Annu. Rev. Pathol.* **2008**, *3*, 399.
- (5) Chong, W. C.; Shastri, M. D.; Eri, R. Endoplasmic Reticulum Stress and Oxidative Stress: A Vicious Nexus Implicated in Bowel Disease Pathophysiology. *Int. J. Mol. Sci.* **2017**, *18*, 771.
- (6) Qun Chena, A. S., Jeremy Thompsona, Ying Hua, Anindita Dasa, Belinda Willardd, Edward J. Lesnefsky. Endoplasmic reticulum stress-mediated mitochondrial dysfunction in aged hearts. *Biochim. Biophys. Acta. Mol. Basis Dis.* **2020**, *1866*, 165899.
- (7) Doyle, K. M.; Kennedy, D.; Gorman, A. M.; Gupta, S.; Healy, S. J.; Samali, A. Unfolded proteins and endoplasmic reticulum stress in neurodegenerative disorders. *J. Cell Mol. Med.* **2011**, *15*, 2025.
- (8) Fonseca, S. G.; Burcin, M.; Gromada, J.; Urano, F. Endoplasmic reticulum stress in beta-cells and development of diabetes. *Curr. Opin. Pharmacol.* **2009**, *9*, 763.
- (9) Scheuner, D.; Kaufman, R. J. The unfolded protein response: a pathway that links insulin demand with beta-cell failure and diabetes. *Endocr. Rev.* **2008**, *29*, 317.
- (10) Calabresi, P.; Mechelli, A.; Natale, G.; Volpicelli-Daley, L.; Di Lazzaro, G.; Ghiglieri, V. Alpha-synuclein in Parkinson's disease and other synucleinopathies: from overt neurodegeneration back to early synaptic dysfunction. *Cell Death Dis.* **2023**, *14*, 176.
- (11) Lindholm, D.; Wootz, H.; Korhonen, L. ER stress and neurodegenerative diseases.

Cell Death Differ. **2006**, *13*, 385.

(12) Cao, S. S.; Kaufman, R. J. Endoplasmic reticulum stress and oxidative stress in cell fate decision and human disease. *Antioxid. Redox Signal.* **2014**, *21*, 396.

(13) Mehtap, K.; Ezgi, O. Endoplasmic Reticulum Stress-Mediated Cell Death. In *Programmed Cell Death*, Hala, G.-M., Omar Nasser, R. Eds.; IntechOpen, 2019; p Ch. 3.

(14) Hetz, C. The unfolded protein response: controlling cell fate decisions under ER stress and beyond. *Nat. Rev. Mol. Cell Biol.* **2012**, *13*, 89.

(15) Alshareef, M. H.; Hartland, E. L.; McCaffrey, K. Effectors Targeting the Unfolded Protein Response during Intracellular Bacterial Infection. *Microorganisms* **2021**, *9*, 705.

(16) Jin, S.-P.; Chung, Jin H. Inhibition of N-glycosylation by tunicamycin attenuates cell-cell adhesion via impaired desmosome formation in normal human epidermal keratinocytes. *Biosci. Rep.* **2018**, *38*, 164.

(17) Siwecka, N.; Rozpedek-Kamińska, W.; Wawrzyńkiewicz, A.; Pytel, D.; Diehl, J. A.; Majsterek, I. The Structure, Activation and Signaling of IRE1 and Its Role in Determining Cell Fate. *Biomed.* **2021**, *9*, 156.

(18) Madden, E.; Logue, S. E.; Healy, S. J.; Manie, S.; Samali, A. The role of the unfolded protein response in cancer progression: From oncogenesis to chemoresistance. *Biol. Cell.* **2019**, *111*, 1.

(19) Hetz, C.; Zhang, K.; Kaufman, R. J. Mechanisms, regulation and functions of the unfolded protein response. *Nat. Rev. Mol. Cell Biol.* **2020**, *21*, 421.

(20) Carreras-Sureda, A.; Pihán, P.; Hetz, C. Calcium signaling at the endoplasmic reticulum: fine-tuning stress responses. *Cell Calcium* **2018**, *70*, 24.

(21) Paul F. Lebeau, K. P., Jae Hyun Byun, and Richard C. Austin. Calcium as a reliable marker for the quantitative assessment of endoplasmic reticulum stress in live cells. *J. Biol. Chem.* **2020**.

(22) Preissler, S.; Rato, C.; Yan, Y.; Perera, L. A.; Czako, A.; Ron, D. Calcium depletion challenges endoplasmic reticulum proteostasis by destabilising BiP-substrate complexes. *eLife* **2020**, *9*, 62601.

(23) Ana M. Rossi, C. W. T. Reliable measurement of free Ca²⁺ concentrations in the ER lumen using Mag-Fluo-4. *Cell Calcium* **2020**, *87*.

- (24) Wang, S.; Zheng, W.; Liu, X.; Xue, P.; Jiang, S.; Lu, D.; Zhang, Q.; He, G.; Pi, J.; Andersen, M. E.; et al. Iodoacetic Acid Activates Nrf2-Mediated Antioxidant Response in Vitro and in Vivo. *Environ. Sci.* **2014**, *48*, 13478.
- (25) Chang, Y. S.; Chang, Y. C.; Chen, P. H.; Li, C. Y.; Wu, W. C.; Kao, Y. H. MicroRNA-100 Mediates Hydrogen Peroxide-Induced Apoptosis of Human Retinal Pigment Epithelium ARPE-19 Cells. *Pharm. (Basel)* **2021**, *14*, 314.
- (26) Kim, D.; Kim, H.; Kim, K.; Roh, S. The Protective Effect of Indole-3-Acetic Acid (IAA) on H₂O₂-Damaged Human Dental Pulp Stem Cells Is Mediated by the AKT Pathway and Involves Increased Expression of the Transcription Factor Nuclear Factor-Erythroid 2-Related Factor 2 (Nrf2) and Its Downstream Target Heme Oxygenase 1 (HO-1). *Oxid. Med. Cell Longev.* **2017**, *2017*, 8639485.
- (27) Poljsak, B.; Šuput, D.; Milisav, I. Achieving the balance between ROS and antioxidants: when to use the synthetic antioxidants. *Oxid. Med. Cell Longev.* **2013**, *2013*, 956792.
- (28) Kovalevich, J.; Langford, D. Considerations for the use of SH-SY5Y neuroblastoma cells in neurobiology. *Methods Mol. Biol.* **2013**, *1078*, 9.
- (29) Shipley, M. M.; Mangold, C. A.; Szpara, M. L. Differentiation of the SH-SY5Y Human Neuroblastoma Cell Line. *J. Vis. Exp.* **2016**, *108*, 53193.
- (30) Shankar, K.; Mehendale, H. M. Oxidative Stress. In *Encyclopedia of Toxicology (Third Edition)*, Wexler, P. Ed.; Academic Press, 2014; pp 735.
- (31) Forman, H. J., Zhang, H. Targeting oxidative stress in disease: promise and limitations of antioxidant therapy. *Nat Rev Drug Discov* **2021**, *20*, 689.
- (32) Lin, J. H.; Walter, P.; Yen, T. S. Endoplasmic reticulum stress in disease pathogenesis. *Annu. Rev. Pathol.* **2008**, *3*, 399.
- (33) Frusciante, L.; Carli, P.; Ercolano, M. R.; Pernice, R.; Di Matteo, A.; Fogliano, V.; Pellegrini, N. Antioxidant nutritional quality of tomato. *Mol. Nutr. Food Res.* **2007**, *51* (5), 609.
- (34) Rao, P. V.; Gan, S. H. Cinnamon: a multifaceted medicinal plant. *Evid. Based Complement Alternat. Med.* **2014**, *2014*, 642942.
- (35) Krobthong, S.; Choowongkamon, K.; Suphakun, P.; Kuaprasert, B.; Samutrtai, P.; Yingchutrakul, Y. The anti-oxidative effect of Lingzhi protein hydrolysates on

lipopolysaccharide-stimulated A549 cells. *Food Biosci.* **2021**, *41*, 101093.

(36) González-Ibáñez, L.; Meneses, M. E.; Sánchez-Tapia, M.; Pérez-Luna, D.; Torres, N.; Torre-Villalvazo, I.; Bonilla, M.; Petlascalco, B.; Castillo, I.; López-Barradas, A.; et al. Edible and medicinal mushrooms (*Pleurotus ostreatus*, *Ustilago maydis*, *Ganoderma lucidum*) reduce endoplasmic reticulum stress and inflammation in adipose tissue of obese Wistar rats fed with a high fat plus saccharose diet. *Food Funct.* **2023**, *14*, 5048.

(37) Rao, R. V.; Bredesen, D. E. Misfolded proteins, endoplasmic reticulum stress and neurodegeneration. *Curr. Opin. Cell Biol.* **2004**, *16*, 653.

(38) Ibe, N. U.; Subramanian, A.; Mukherjee, S. Non-canonical activation of the ER stress sensor ATF6 by *Legionella pneumophila* effectors. *Life Sci. Alliance* **2021**, *4*, 1247.

(39) Yoshida, H.; Matsui, T.; Yamamoto, A.; Okada, T.; Mori, K. XBP1 mRNA is induced by ATF6 and spliced by IRE1 in response to ER stress to produce a highly active transcription factor. *Cell* **2001**, *107*, 881.

(40) Rozpedek, W.; Pytel, D.; Mucha, B.; Leszczynska, H.; Diehl, J. A.; Majsterek, I. The Role of the PERK/eIF2 α /ATF4/CHOP Signaling Pathway in Tumor Progression During Endoplasmic Reticulum Stress. *Curr. Mol. Med.* **2016**, *16*, 533.

(41) Adams, C. J.; Kopp, M. C.; Larburu, N.; Nowak, P. R.; Ali, M. M. U. Structure and Molecular Mechanism of ER Stress Signaling by the Unfolded Protein Response Signal Activator IRE1. *Front. Mol. Biosci.* **2019**, *6*, 11.

(42) Molinari, M.; Eriksson, K. K.; Calanca, V.; Galli, C.; Cresswell, P.; Michalak, M.; Helenius, A. Contrasting Functions of Calreticulin and Calnexin in Glycoprotein Folding and ER Quality Control. *Mol. Cell* **2004**, *13*, 125.

(43) Sehgal, P.; Szalai, P.; Olesen, C.; Praetorius, H. A.; Nissen, P.; Christensen, S. B.; Engedal, N.; Møller, J. V. Inhibition of the sarco/endoplasmic reticulum (ER) Ca²⁺-ATPase by thapsigargin analogs induces cell death via ER Ca²⁺ depletion and the unfolded protein response. *J. Biol. Chem.* **2017**, *292*, 19656.

(44) Jin, S. P.; Chung, J. H. Inhibition of N-glycosylation by tunicamycin attenuates cell-cell adhesion via impaired desmosome formation in normal human epidermal keratinocytes. *Biosci. Rep.* **2018**, *38*, 1641.

(45) Yang Wang, L. Z., Zhiyan He, Jiong Deng; , Z. Z., Liu Liu, Weimin Ye, Shuli Liu.

Tunicamycin induces ER stress and inhibits tumorigenesis of head and neck cancer cells by inhibiting N-glycosylation. *Am. J. Transl. Res.* **2022**, *12*, 541.

(46) Yingchutrakul, Y.; Krobthong, S.; Choowongkomon, K.; Papan, P.; Samutrtai, P.; Mahatnirunkul, T.; Chomtong, T.; Srimongkolpithak, N.; Jaroenchuensiri, T.; Aonbangkhen, C. Discovery of a Multifunctional Octapeptide from Lingzhi with Antioxidant and Tyrosinase Inhibitory Activity. In *J. Pharm.*, **2022**, *15*, 684.

(47) Krobthong, S.; Yingchutrakul, Y.; Sittisaree, W.; Tulyananda, T.; Samutrtai, P.; Choowongkomon, K.; Lao-On, U. Evaluation of potential anti-metastatic and antioxidative abilities of natural peptides derived from *Tecoma stans* (L.) Juss. ex Kunth in A549 cells. *PeerJ* **2022**, *10*, 13693.

(48) Matemu, A.; Nakamura, S.; Katayama, S. Health Benefits of Antioxidative Peptides Derived from Legume Proteins with a High Amino Acid Score. *Antioxidants* **2021**, *10* (2).

(49) Gerlier, D.; Thomasset, N. Use of MTT colorimetric assay to measure cell activation. *J. Immunol. Methods* **1986**, *94*, 57.

(50) Badr, M.; Wolfgang; Trommer, W. The ribosome-inactivating protein gelonin and parts thereof to be employed for a potential treatment of cancer. *J. Toxins* **2023**, *2*, 2699.

(51) El-Sharkawey, A. Calculate the Corrected Total Cell Fluorescence (CTCF). 2016.

(52) Wang, W.; Kang, P. M. Oxidative Stress and Antioxidant Treatments in Cardiovascular Diseases. *Antioxidants (Basel)* **2020**, *9* (12), 1292.

(53) Barnham, K. J.; Masters, C. L.; Bush, A. I. Neurodegenerative diseases and oxidative stress. *Nat. Rev. Drug Discov.* **2004**, *3* (3), 205.

(54) Schneider, E. M.; Sievers, A. Concanavalin A binds to the endoplasmic reticulum and the starch grain surface of root statocytes. *Planta* **1981**, *152* (3), 177.

(55) company, H. a. P. *PhenoVue™ cellular membrane/ER stain (Concanavalin A)*. <https://horizondiscovery.com/>.

(56) Yuan, H.; Zhao, Z.; Guo, Z.; Ma, L.; Han, J.; Song, Y. A Novel ER Stress Mediator TMTC3 Promotes Squamous Cell Carcinoma Progression by Activating GRP78/PERK Signaling Pathway. *Int. J. Biol. Sci.* **2022**, *18*, 4853.



จุฬาลงกรณ์มหาวิทยาลัย
CHULALONGKORN UNIVERSITY

APPENDIX

Table 1. Standard anticancer drug (Etoposide) testing in SH-SY5Y and L929 cells.

Concentration (μM)	% Viability			
	%Viability (SH-SY5Y)	SD	%Viability (L929)	SD
12.5 μM	68.4333	2.7875	83.9241	3.8880
25 μM	58.2915	1.1764	80.6163	4.4176
50 μM	52.5668	0.5276	77.4795	6.0489
125 μM	43.8172	1.6532	68.3032	6.2382
250 μM	38.6585	2.5832	60.4912	6.6474
500 μM	26.9709	1.4764	44.4567	4.7939

Table 2. Toxicity of the 25, 50, and 100 $\mu\text{g}/\text{mL}$ peptide hydrolysates from riceberry rice (SH-SY5Y cells).

Concentration ($\mu\text{g}/\text{mL}$)	25		50		100	
	%Viability	SD	%Viability	SD	%Viability	SD
Untreated	100	0	100	0	100	0
ID 1	93.9790	3.2891	99.5617	3.1929	103.079	8.3387
ID 2	94.9640	0.9112	99.7727	5.1181	110.010	6.2317
ID 3	94.8010	2.5435	100.346	7.6113	114.451	6.6393
ID 4	94.8010	3.6914	97.3924	7.9574	112.836	6.8120
ID 5	95.8085	2.4870	99.5929	4.2525	110.724	7.0594
ID 6	95.3429	5.6629	94.9991	3.8057	101.319	6.3513
ID 7	95.1676	4.5156	96.9038	5.5440	100.015	1.2053
ID 8	95.2831	3.2332	97.9115	7.1085	99.0689	1.3462
ID 9	96.7336	4.4839	96.1186	2.4577	97.5347	4.6735
ID 10	99.7695	6.4986	96.7153	3.2355	94.6516	8.4807

Table 3. Determining the appropriate concentration of IAA to induce oxidative stress in cells (SH-SY5Y cells).

Incubation Time	1 h.		2 h.		3 h.	
	%Viability	SD	%Viability	SD	%Viability	SD
Concentration (μM)						
25	94.0341	3.4510	90.5837	2.5716	86.3762	5.1115
50	93.8920	5.9519	91.3619	1.2858	69.6750	5.1346
100	83.6648	3.7414	84.3580	1.0527	68.2780	1.1426
200	76.7045	3.0950	81.2451	3.7378	66.7914	3.10742
500	81.1790	0.3690	81.4008	4.0504	35.1314	0.7187

Table 4. Determining the appropriate concentration of H_2O_2 to induce oxidative stress in cells (SH-SY5Y cells).

Concentration (μM)	%Viability	SD
500	60.1758	8.9310
1000	19.2855	0.5432
2000	19.3677	2.1587

Table 5. Antioxidant activity of riceberry rice peptides at 25, 50 $\mu\text{g}/\text{mL}$ against IAA 200 μM (SH-SY5Y).

Concentration (μM)	25		50	
	Viability	SD	Viability	SD
Untreated	100	0	100	0
IAA alone	70.5685	3.9199	76.2380	1.5968
ID 1	69.8395	2.6584	71.6281	2.1867
ID 2	76.3602	4.9955	77.6419	0.9337
ID 3	80.1895	1.7433	80.3149	1.5128
ID 4	79.6035	1.8685	79.3901	3.3406
ID 5	78.3167	2.8687	80.2958	3.6137
ID 6	76.8172	1.7683	75.2126	1.1719
ID 7	77.2442	2.7973	76.1947	1.4477
ID 8	74.4761	2.8875	71.8207	2.6693
ID 9	74.4758	4.8273	71.4838	3.4225
ID 10	71.3478	0.6062	77.2117	5.8450

Table 6. Antioxidant activity of riceberry rice peptides at 25, 50, and 100 $\mu\text{g/mL}$ against with IAA 500 μM (SH-SY5Y).

Concentration ($\mu\text{g/mL}$)	25		50		100	
	Viability	SD	Viability	SD	Viability	SD
Untreated	100	0	100	0	100	0
IAA alone	43.3435	2.1080	43.5615	1.8634	35.0341	1.6079
ID 1	41.0166	5.6653	35.5424	0.9023	40.4545	4.5238
ID 2	44.0862	1.2743	40.5646	4.6962	44.0122	2.7834
ID 3	48.0646	2.0661	45.3513	1.1189	47.7832	5.6613
ID 4	47.9397	2.4003	46.4406	0.5193	46.0370	1.6830
ID 5	48.7132	2.8084	47.9819	3.1766	46.5201	2.3605
ID 6	48.3117	2.2453	44.5653	3.3888	44.8551	3.1257
ID 7	49.0750	3.6517	44.3049	3.5743	45.3768	2.8021
ID 8	48.9088	2.7963	44.7175	3.7593	45.7992	3.4317
ID 9	48.8568	1.5418	44.1421	4.5854	45.7780	1.3800
ID 10	48.2214	1.4058	44.444	2.5070	45.2841	2.1246

Table 7. Investigating the effectiveness of 25 and 50 $\mu\text{g/mL}$ of peptides in mitigating oxidative stress induced by H_2O_2 at a concentration of 500 μM (SH-SY5Y cells).

Concentration ($\mu\text{g/mL}$)	25		50	
	Viability	SD	Viability	SD
Untreated	100	0	100	0
IAA alone	77.0095	10.6247	83.0867	2.5631
ID 1	75.0523	10.3113	85.0938	3.0950
ID 2	77.0206	7.4223	87.5121	1.8206
ID 3	80.2049	5.3319	89.9899	3.1370
ID 4	80.2983	10.4944	91.3148	1.5130
ID 5	81.0975	7.4061	90.0280	3.2290
ID 6	78.7563	4.8613	86.4992	3.6803
ID 7	78.0941	8.8019	87.8568	4.4846
ID 8	80.6665	8.2816	86.2102	4.8396
ID 9	79.8035	6.6624	88.4342	3.4780
ID 10	82.2926	9.8977	90.2752	0.6772

Table 8. Toxicity of the 50 $\mu\text{g/mL}$ peptide hydrolysates from riceberry rice (L929 cells).

Concentration ($\mu\text{g/mL}$)	50	
	%Viability	SD
ID 1	90.1931	5.2041
ID 2	97.9088	4.2675
ID 3	94.8058	2.8052
ID 4	91.2052	4.0287
ID 5	94.6602	3.4799
ID 6	94.9074	3.5162
ID 7	89.8283	3.1626
ID 8	92.1442	5.0503
ID 9	85.1687	3.9884
ID 10	98.8033	1.9959

Table 9. Antioxidant activity of riceberry rice peptides 50 and 100 $\mu\text{g}/\text{mL}$ against IAA 500 μM in L929 cells.

Concentration ($\mu\text{g}/\text{mL}$)	50		100	
	%Viability	SD	%Viability	SD
Untreated	100	0	100	0
IAA alone	39.0367	2.0010	55.0341	1.6079
ID 1	29.7256	2.7332	60.4545	4.5238
ID 2	35.7334	3.0710	64.0122	2.7834
ID 3	40.7213	0.8747	67.7832	5.6613
ID 4	43.7204	4.2393	67.0011	0.2979
ID 5	44.7476	4.8009	67.2033	1.5572
ID 6	42.8170	3.8064	64.8551	3.1257
ID 7	42.8109	4.6492	65.3768	2.8021
ID 8	42.0122	4.2343	65.7992	3.4317
ID 9	42.9695	3.6740	65.7780	1.3799
ID 10	39.1393	4.8289	65.2841	2.1246

Table 10. Investigating the effectiveness of 50 µg/mL of peptides in mitigating oxidative stress induced by H₂O₂ at a concentration of 500 µM (L929 cells).

Concentration (µg/mL)	50	
	%Viability	SD
Untreated	100	0
H ₂ O ₂ alone	88.7766	2.4299
ID 1	94.6730	3.3491
ID 2	94.6843	2.8083
ID 3	97.6238	1.6510
ID 4	98.2211	0.4025
ID 5	97.3509	1.8005
ID 6	93.5029	2.1552
ID 7	91.3436	4.3309
ID 8	95.4374	4.0106
ID 9	92.1989	3.0156
ID 10	96.4736	2.4181

VITA

NAME Theeranuch Jaroenchuensiri

DATE OF BIRTH 4 Dec 1998

PLACE OF BIRTH Bangkok, Thailand

INSTITUTIONS ATTENDED Bachelor's Degree in Chemistry, Chulalongkorn University (2560-2563)
Master's Degree in Green Chemistry and Sustainability Chemistry, Chulalongkorn University (2564-Present)

HOME ADDRESS 165/96 Kanda village, Soi Bangkhae10, Sukhapiban1 Rd., Bangkhae, Bangkhae, Bangkok

PUBLICATION The 40th International Conference of the Microscopy Conference of the Microscopy Society of Thailand (MST40)